CENTER FOR TOKAMAK TRANSIENTS SIMULATION

CTTS Physics Overview

Stephen C. Jardin

SciDAC-4 PI Meeting

Virtual

October 22, 2021

CTTS Participants

PHYSICS TEAM

- **PPPL**: C. Clauser, N. Ferraro, I. Krebs, S. Jardin, C. Liu, D. Pfefferlie ,C. Zhao
- **GA**: C. Kim ,L. Lao, B. Lyons, J. McClenaghan, P. Parks
- **U. Wisc**: K. Bunkers, B. Cornille , , A. Sainterme , C. Sovinec, G. Wang , P. Zhu
- **Utah State U**: E. Held, J.Ji, A. Spenser, T. Taylor, T. Markham, H. Lee, B. Adair
- **Tech X:** E. Howell, J. King, S. Kruger
- **SBU:** R. Samulyak
- **HRS Fusion**: H. Strauss

HPC TEAM

- **RPI**: U. Riaz, S. Seol, M. Shephard, M. Siboni
- **LBL:** N. Ding, X. Li, Y. Liu, S. Williams
- **PPPL**: J. Chen
- **SBU**: N. Naitlho, R. Samulyak, S. Yuan

41 participants
9 institutions

Center for Tokamak Transient Simulations -- Outline

1. Code Descriptions and code benchmarks
2. Forces due to Vertical Displacement Events
3. Disruption Mitigation via Impurity Injections
4. Runaway Electrons interacting with MHD
5. Neoclassical Tearing Modes and Mode Locking
6. Sawteeth and Sawtooth-free discharges
7. Soft beta limits and disruption avoidance
8. List of talks at 2021 Theory and Simulation of Disruption Workshop
9. Publications
10. Summary
11. Future Plans

Center for Tokamak Transient Simulations -- Outline

1. Code Descriptions and code benchmarks

   ASCR Presentations

2. Forces due to Vertical Displacement Events
3. Disruption Mitigation via Impurity Injections
4. Runaway Electrons interacting with MHD
5. Neoclassical Tearing Modes and Mode Locking
6. Sawteeth and Sawtooth-free discharges
7. Soft beta limits and disruption avoidance
8. List of talks at 2021 Theory and Simulation of Disruption Workshop
9. Publications
10. Summary
11. Future Plans

Center for Tokamak Transient Simulations -- Outline

1. Code Descriptions and code benchmarks
2. Forces due to Vertical Displacement Events
3. Disruption Mitigation via Impurity Injections
4. Runaway Electrons interacting with MHD
5. Neoclassical Tearing Modes and Mode Locking
6. Sawteeth and Sawtooth-free discharges
7. Soft beta limits and disruption avoidance
8. List of talks at 2021 Theory and Simulation of Disruption Workshop
9. Publications
10. Summary
11. Future Plans

M3D-C¹ and NIMROD solve 3D MHD Equations in Toroidal Geometry including Impurity Radiation and Runaway Electrons

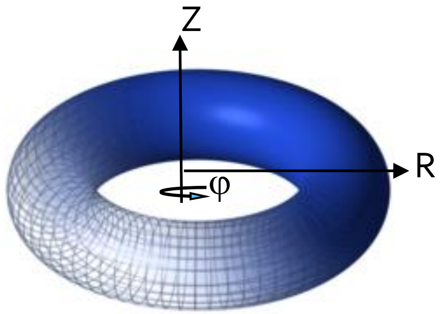

$$\partial n_i/\partial t + \nabla \bullet (n_i \mathbf{V}) = \nabla \bullet D \nabla n_i + S_n$$

$$\partial n_Z^{(j)}/\partial t + \nabla \bullet (n_Z^{(j)} \mathbf{V}) = \nabla \bullet D \nabla n_Z^{(j)} + I_Z^{(j-1)} n_Z^{(j-1)} - \left(I_Z^{(j)} + R_Z^{(j)} \right) n_Z^{(j)} + R_Z^{(j+1)} n_Z^{(j+1)} + S_Z^{(j)}$$

$$\left.\begin{array}{c} \partial \mathbf{A}/\partial t = -\mathbf{E} - \nabla \Phi \\ \nabla_\perp \bullet \dfrac{1}{R^2} \nabla \Phi = -\nabla_\perp \bullet \dfrac{1}{R^2} \mathbf{E} \\ \mathbf{B} = \nabla \times \mathbf{A} \end{array}\right\} \text{M3D-C1} \qquad \left.\begin{array}{c} \partial \mathbf{B}/\partial t = -\nabla \times \mathbf{E} \\ \nabla \bullet \mathbf{B} = 0 \end{array}\right\} \text{NIMROD}$$

$$\rho(\partial \mathbf{V}/\partial t + \mathbf{V} \bullet \nabla \mathbf{V}) + \nabla p = \mathbf{J} \times \mathbf{B} - \nabla \bullet \mathbf{\Pi} - \varpi \mathbf{V} + \mathbf{S}_m, \qquad \mathbf{E} + \mathbf{V} \times \mathbf{B} = \eta(\mathbf{J} - \mathbf{J}_{RA}) + \mathbf{S}_{CD}$$

$$\frac{3}{2}\left[\frac{\partial p_e}{\partial t} + \nabla \bullet \left(p_e \mathbf{V} \right) \right] = -p_e \nabla \bullet \mathbf{V} + \mathbf{J} \bullet \mathbf{E} - \nabla \bullet \mathbf{q}_e + Q_\Delta + S_{eE} \qquad \mathbf{q}_{e,i} = -\kappa_{e,i} \nabla T_{e,i} - \kappa_{\| e,i} \nabla_\| T_{e,i}$$

$$\frac{3}{2}\left[\frac{\partial p_i}{\partial t} + \nabla \bullet \left(p_i \mathbf{V} \right) \right] = -p_i \nabla \bullet \mathbf{V} - \mathbf{\Pi}_i : \nabla \mathbf{V} - \nabla \bullet \mathbf{q}_i - Q_\Delta + \tfrac{1}{2} \varpi V^2 + S_{iE}$$

- Also, separate equations for resistive wall and vacuum regions
- Codes have a fluid model for Runaway Electron current $\mathbf{J}_{RA}$ (with sources)
- Impurity pellet ablation models

M3D-C^1 and NIMROD have very different numerical implementations

	M3D-C^1	**NIMROD**
Poloidal Direction	Tri. C^1 Reduced Quintic FE	High. Order quad C^0 FE
Toroidal Direction	Hermite Cubic C^1 FE	Spectral
Magnetic Field	$\mathbf{B} = \nabla\psi \times \nabla\varphi - \nabla_\perp f' + F\nabla\varphi$	$\mathbf{B} = B_r\widehat{R} + B_z\hat{Z} + B_\varphi\widehat{\varphi}$
Velocity Field	$\mathbf{V} = R^2\nabla U \times \nabla\varphi + \omega R^2\nabla\varphi + R^{-2}\nabla_\perp\chi$	$\mathbf{V} = V_r\widehat{R} + V_z\hat{Z} + V_\varphi\widehat{\varphi}$
Coupling to Conductors	same matrix	Separate matrices w interface

Both codes use:

- Split Implicit time advance
- Block-Jacobi preconditioner based on SuperLU_DIST or MUMPS
- GMRES based iterative solvers
- Impurity ionization and recombination rates from KPRAD

Because the two codes use different representations, but solve the same equations, they are a very good check on one another.

Several "deep dive" verification exercises in the last few years:

Disruption Mitigation in 2D
B.Lyons, et al, "Axisymmetric benchmarks of impurity dynamics in extended-magnetohydrodynamic simulations", Plasma Physics and Controlled Fusion **61** (2019)

VDE in 2D
I. Krebs, et al, "Axisymmetric simulations of vertical displacement events in tokamaks: A benchmark of M3D-C1, NIMROD, and JOREK", Phys Plasmas **27** (2020)

VDE in 3D
F. Artola, et al, "3D simulations of vertical displacement events in tokamaks: A benchmark of M3D-C1, NIMROD, and JOREK", Phys Plasmas **28** (2021)

Disruption Mitigation in 3D
In progress (2021/2022)

Disruption Mitigation in 2D

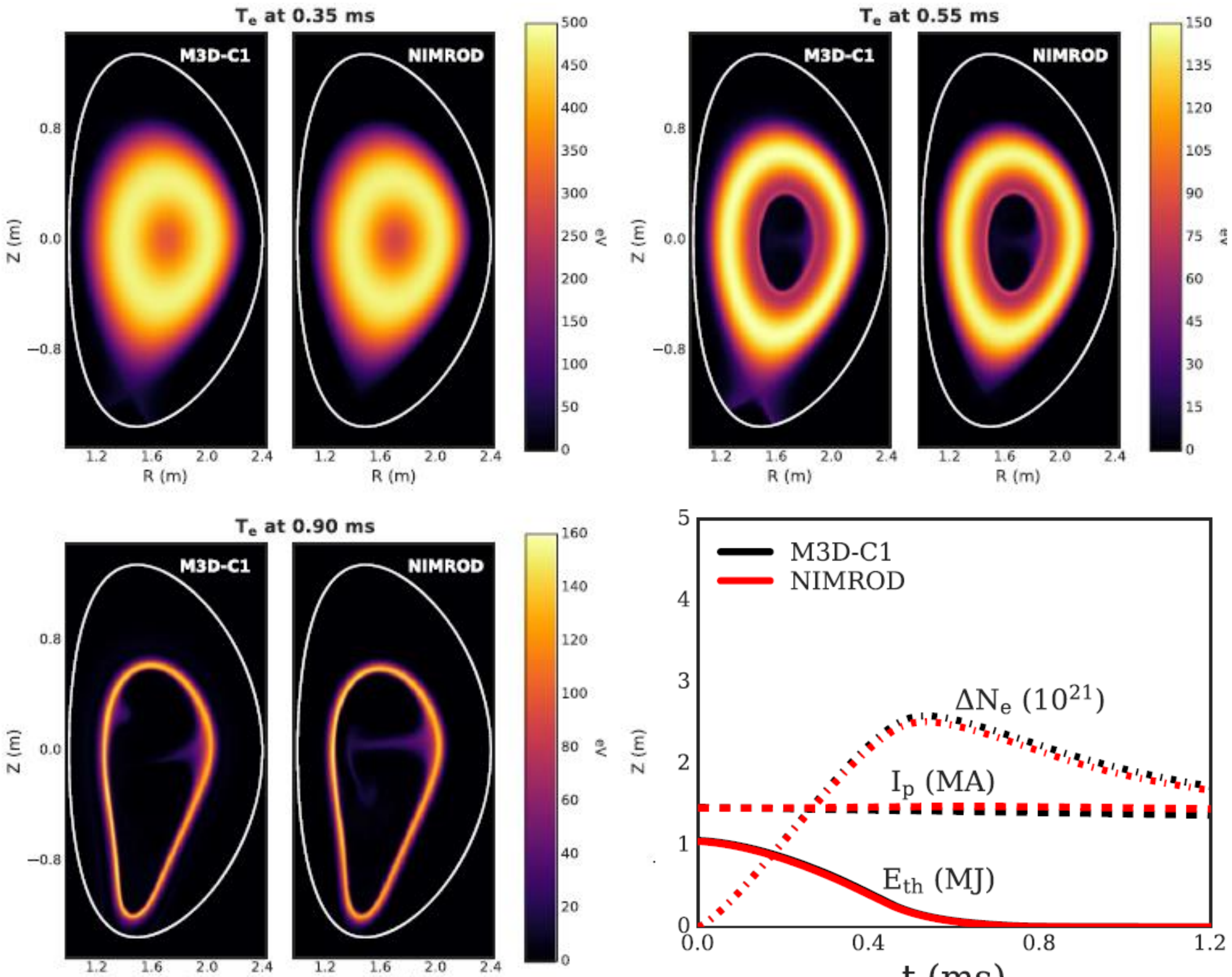

- Code verification exercise starts with realistic DIII-D equilibrium to which argon has been added
- Shown at left are the M3D-C[1] and NIMROD electron temperatures at 3 times during the argon-induced quench. (color scale varies at each time.)
- Also shown and in excellent agreement are the time histories of global plasma quantities such as thermal energy, plasma current, and total number of electrons.
- This provided an invaluable check on both the ionization, radiation, and MHD routines, and several (minor) errors were corrected.

Lyons, Kim et ap, PPCF **61** (2019),

2D Linear VDE benchmark between M3D-C1, NIMROD & JOREK

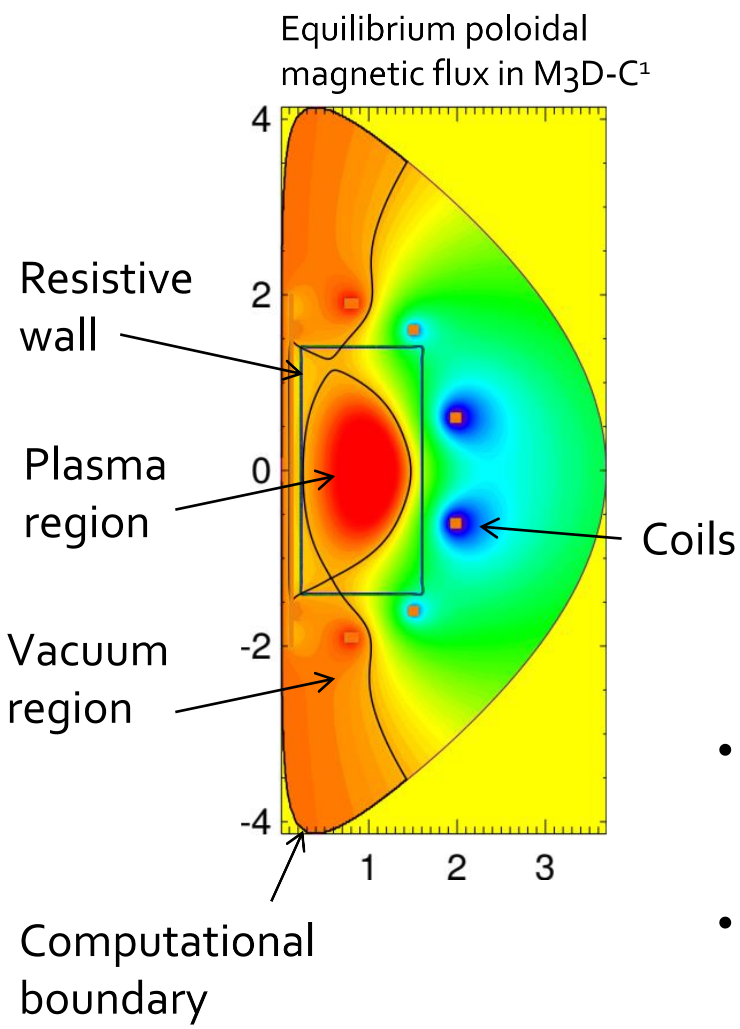

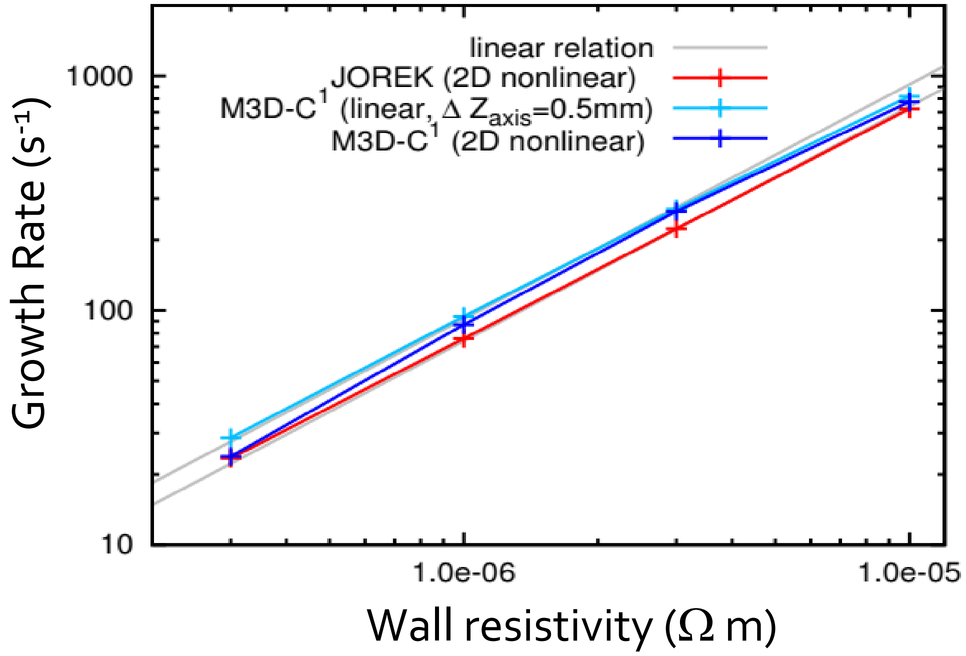

- Realistic equilibrium (NSTX) but simplified geometry that all codes can handle (rectangular resistive wall)
- Codes agree to within a few % on growth rates over wide range of wall resistivity. Excellent check on resistive wall routines

I. Krebs, C. Sovinec, et al, Phys Plasmas **27** (2020)

2D Nonlinear VDE benchmark between M3D-C¹, NIMROD & JOREK

Poloidal magnetic flux

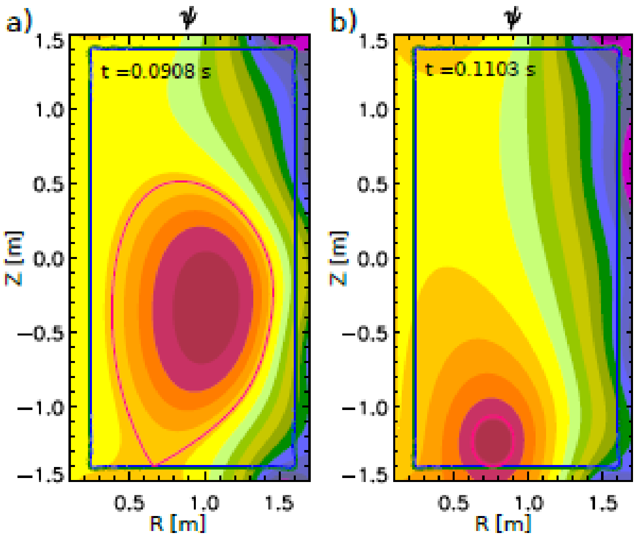

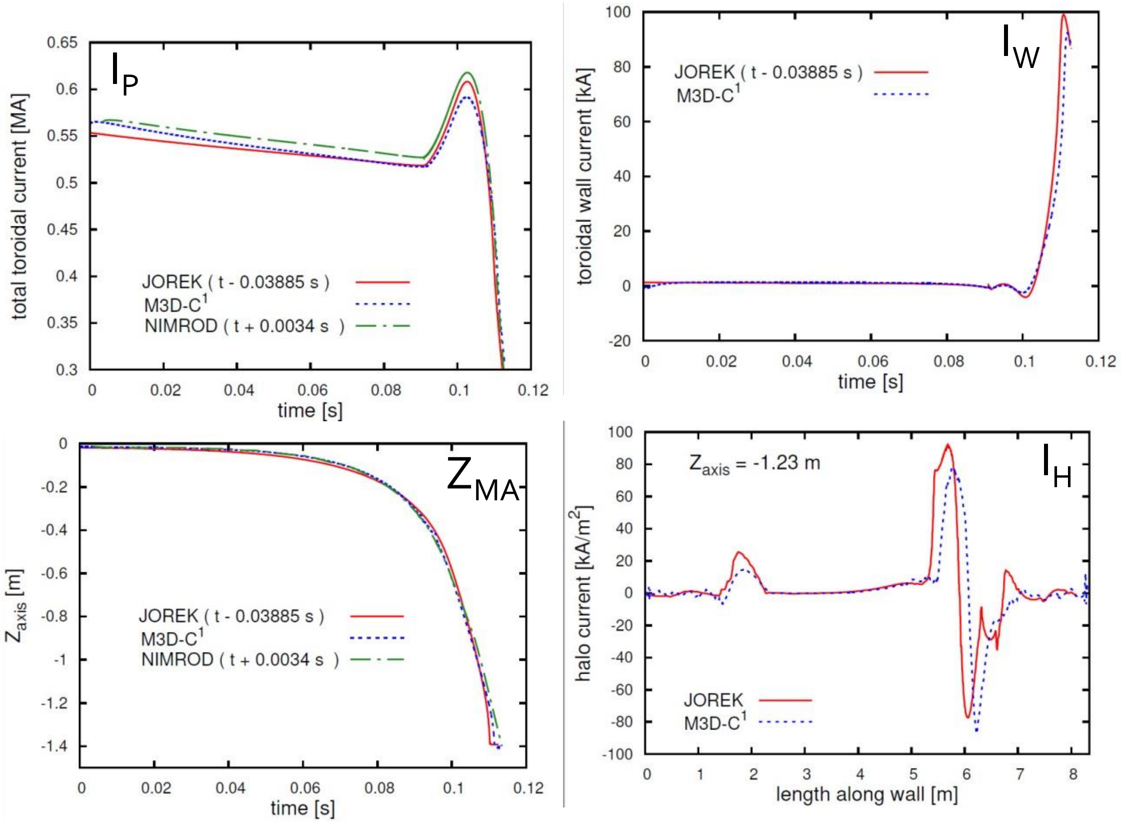

- Good agreement amongst 3 codes on time evolution of plasma and wall currents, plasma position and the halo current distribution.

I. Krebs, C. Sovinec, et al, Phys Plasmas **27** (2020)

3D Nonlinear VDE benchmark between M3D-C¹, NIMROD, and JOREK

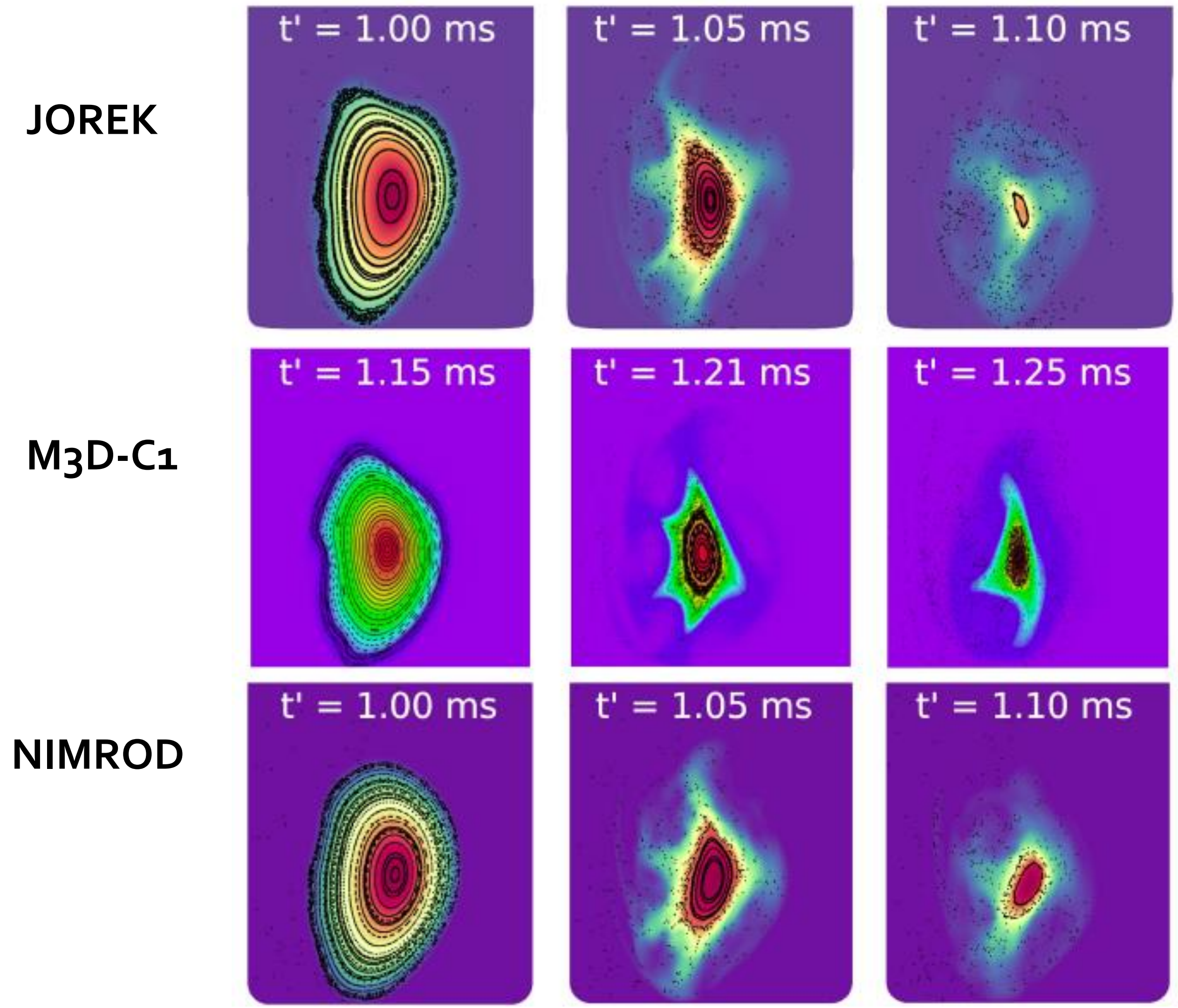

- Shown at left are the evolution of the pressure at plane ϕ=0 for the 3 codes at late times, after n > 0 instabilities have set in. Poincare plots showing the magnetic topology are overlaid.

- Below are the z-position of the magnetic axis and plasma current vs time for the 3 codes

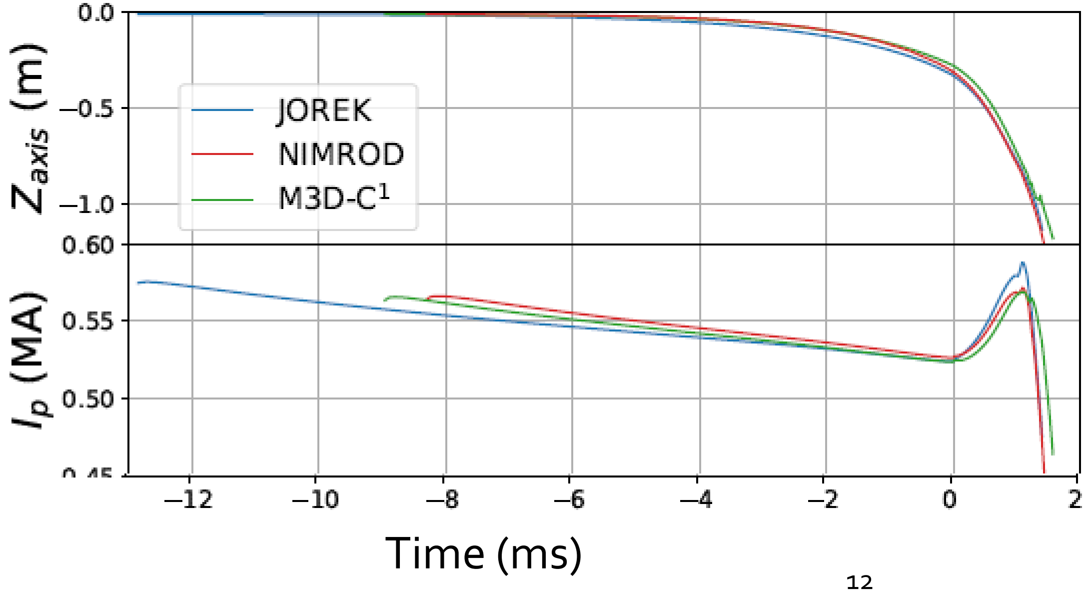

I. F. Artola, et al" Phys Plasmas **28** (2021)

3D Disruption Mitigation Modeling (in progress)

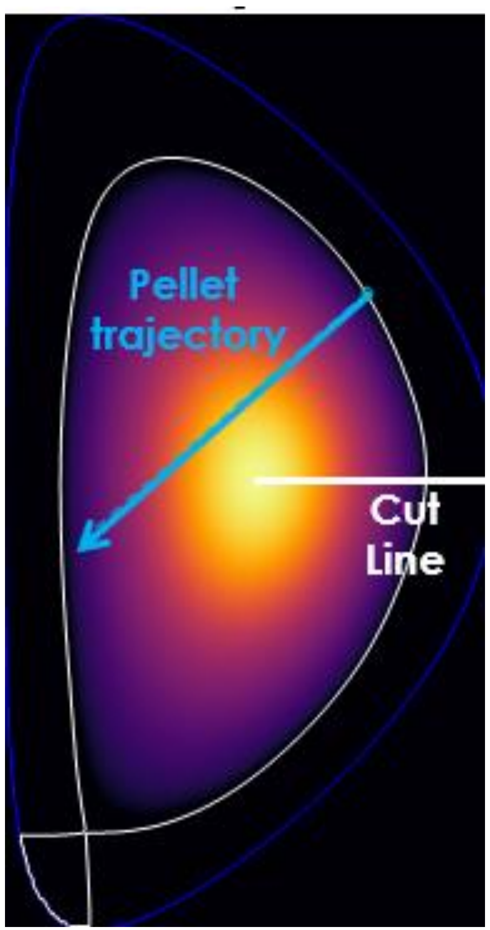

- M3D-C^1 and NIMROD modeling same SPI Mitigation shot on DIII-D for benchmark

- Initial comparisons showed differences near boundary, M3D-C^1 saw return flow on open field lines, NIMROD did not

M3D-C^1

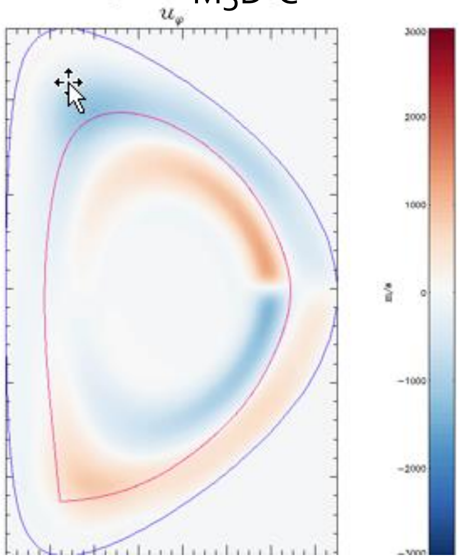

NIMROD

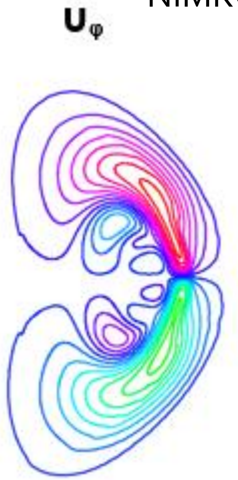

- After much digging, it turned out that M3D-C^1 and NIMROD were implementing the no-slip boundary condition differently at the wall.

- M3D-C^1 was forcing both the stream function and the potential parts of the velocity field to vanish at the boundary, not just their sum

- After this was corrected, the 2 codes agreed much better (next slide)!

Lyons, Kim

M3D-C1 flow fields before and after slip boundary conditions are corrected

before

$$R^2\nabla U\times\nabla\varphi\bullet\hat{t}=0$$

$$R^{-2}\nabla\chi\bullet\hat{t}=0$$

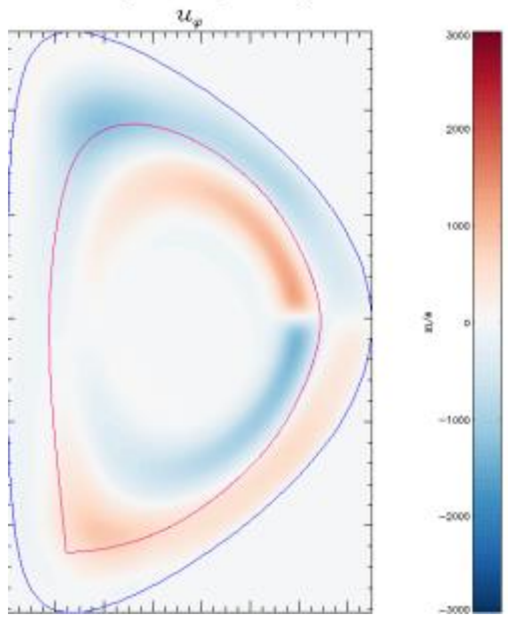

after

$$\left[R^2\nabla U\times\nabla\varphi+R^{-2}\nabla\chi\right]\bullet\hat{t}=0$$

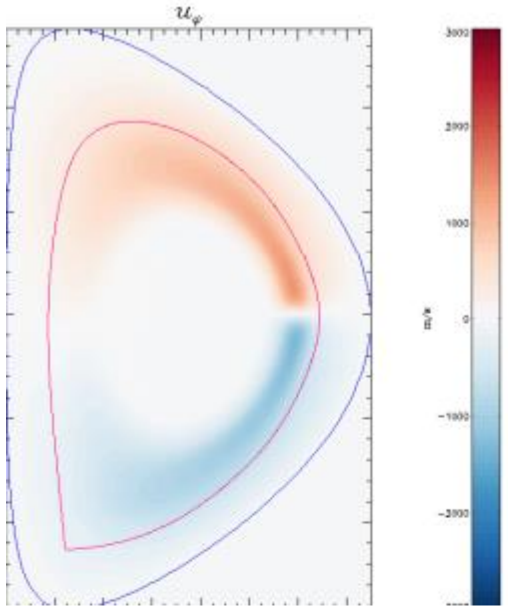

Poloidal flow along midplane cut

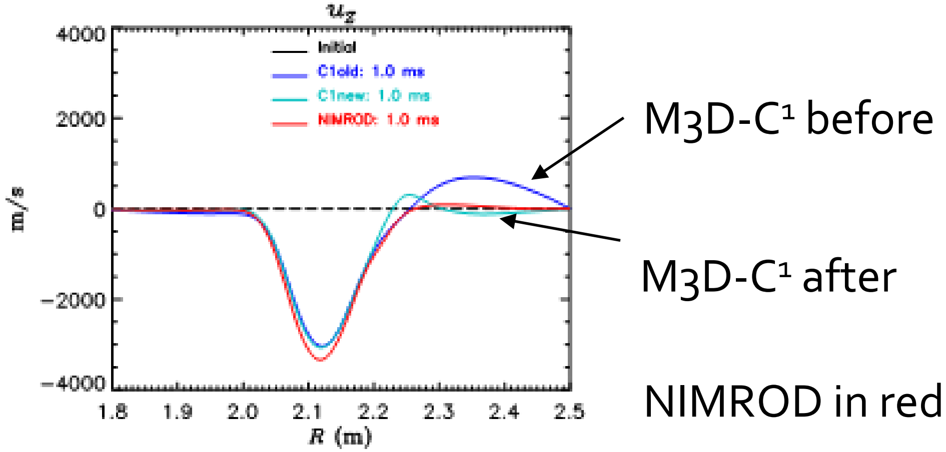

- This “bug” may never have been uncovered if not for this benchmark

Lyons, Kim

Center for Tokamak Transient Simulations -- Outline

1. Code Descriptions and code benchmarks
2. Forces due to Vertical Displacement Events
3. Disruption Mitigation via Impurity Injections
4. Runaway Electrons interacting with MHD
5. Neoclassical Tearing Modes and Mode Locking
6. Sawteeth and Sawtooth-free discharges
7. Soft beta limits and disruption avoidance
8. List of talks at 2021 Theory and Simulation of Disruption Workshop
9. Publications
10. Summary
11. Future Plans

Vertical Displacement Events (VDEs) can occur when vertical position control is lost

- We have calculated the forces to be expected in the ITER vessel in both the vertical and horizontal directions

- The vertical forces can be computed in 2D,but the horizontal require 3D

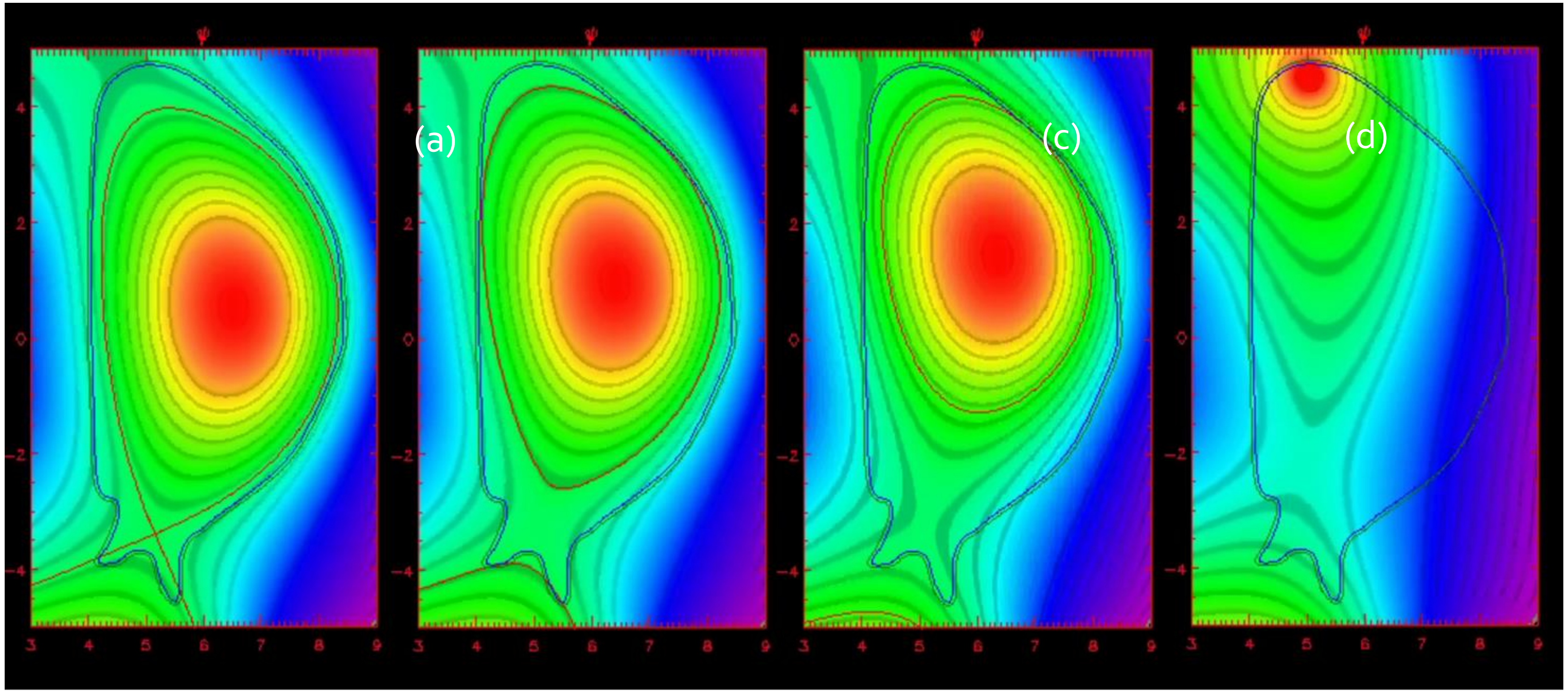

Equilibrium Wall contact Start TQ Final

5.3 T 15MA ITER

I. Krebs

The VDE induces both toroidal and poloidal currents in the vessel, both of which cause large forces due to J x B

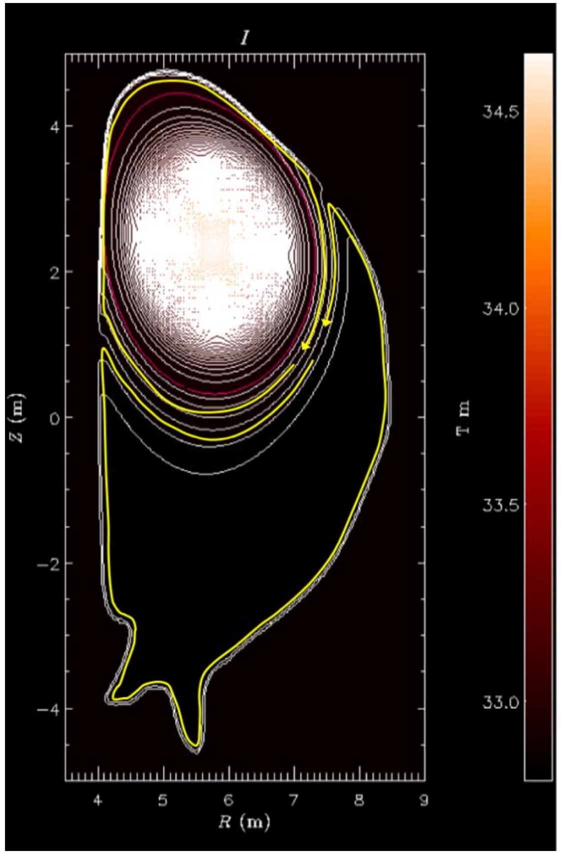

Halo currents (shown in yellow) pass between plasma and structure

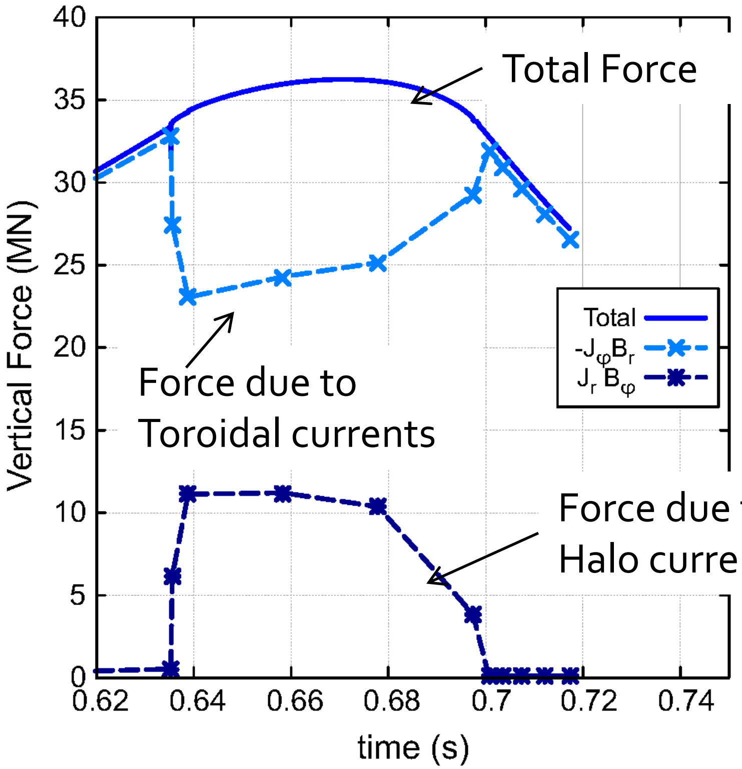

- Plotted are the wall forces arise due both to the toroidal currents (top) and the poloidal halo currents (bottom)
- We found that the large force due to halo currents is compensated by reduced force due to toroidal currents !!

C. Clauser, NF 59 (2019)

The VDE induces both toroidal and poloidal currents in the vessel, both of which cause large forces due to J x B

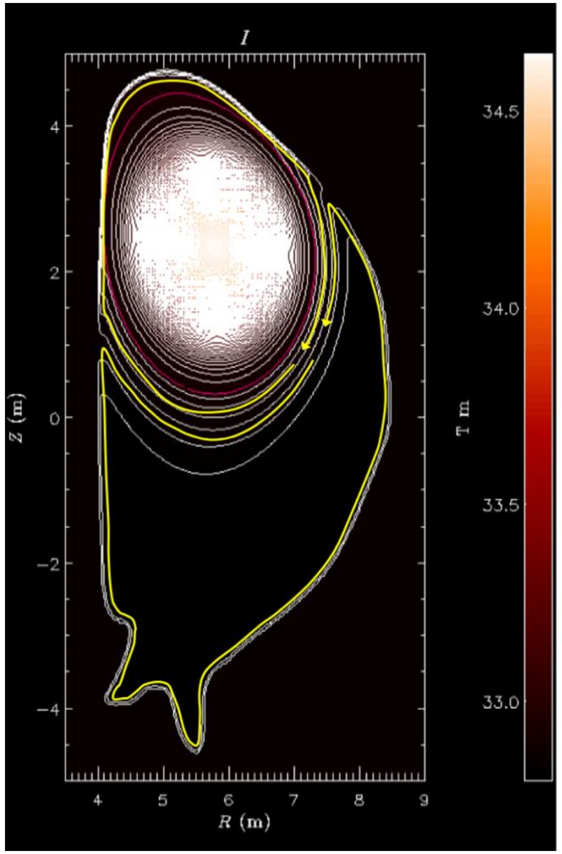

Halo currents (shown in yellow) pass between plasma and structure

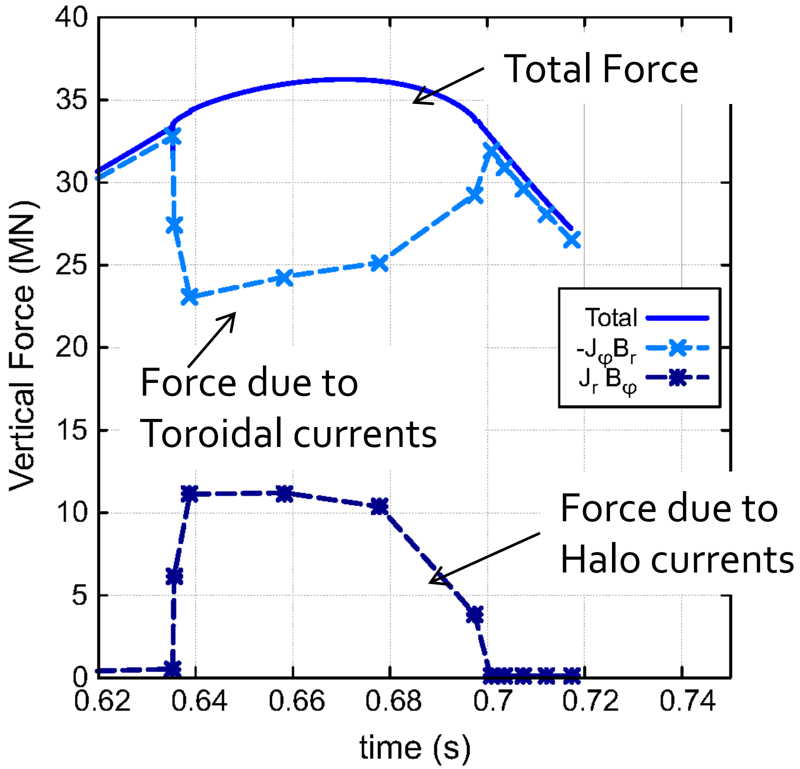

This study provided new insight into the forces due to the halo currents

- Plotted are the wall forces arise due both to the toroidal currents (top) and the poloidal halo currents (bottom)
- We found that the large force due to halo currents is compensated by reduced force due to toroidal currents !!

C. Clauser, NF 59 (2019)

Cold VDE in ITER due to current quench

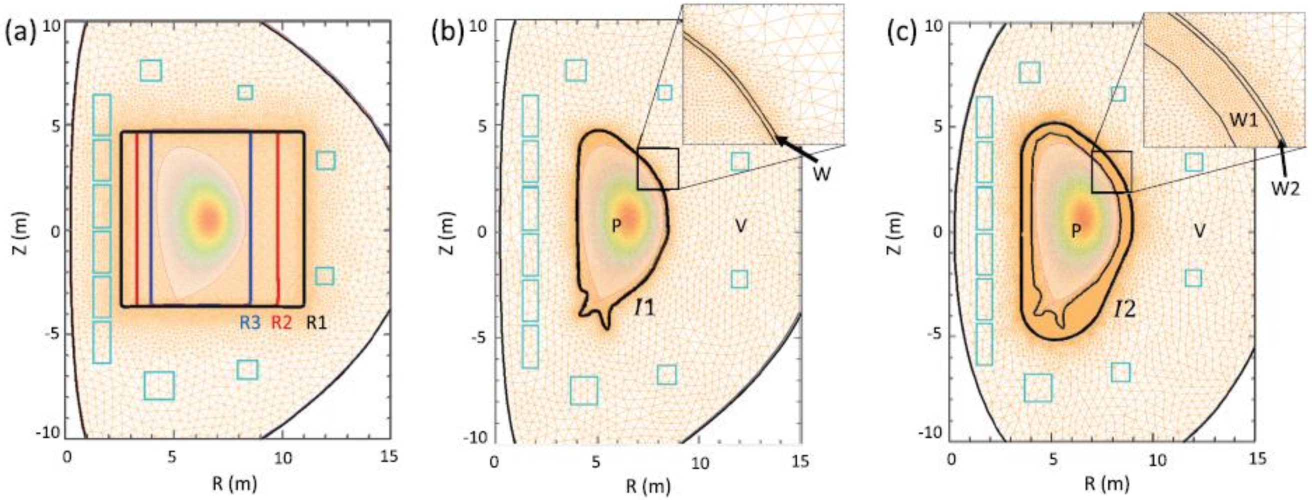

- Alan Boozer wrote a paper claiming that a fast current quench in ITER would cause it to become unstable to a VDE, even if the walls were perfectly conducting

- His analytic analysis made a number of geometrical simplifications (rectangular vv)

- We were able to show that under Boozer's assumptions, we recover his result numerically

- However, extending this to more realistic ITER geometry and parameters, we found that this was not a significant concern for ITER

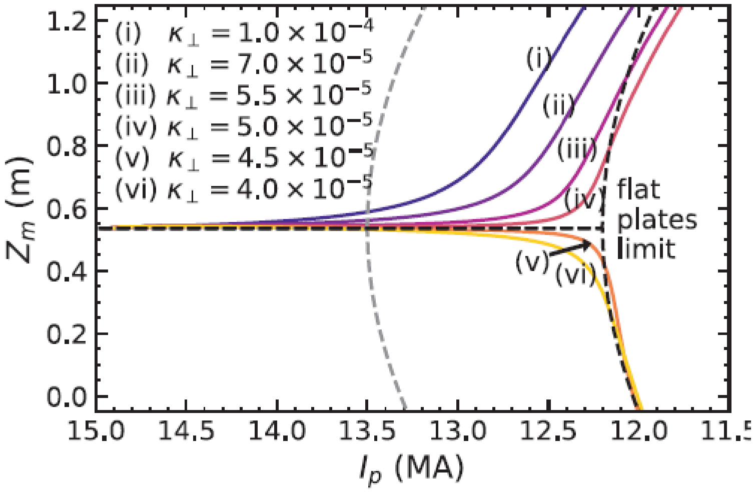

Clauser< Phys Plasma **, 28** (2021)

3D M3D-C¹ simulation of JET VDE shows origin and magnitude of sideways force

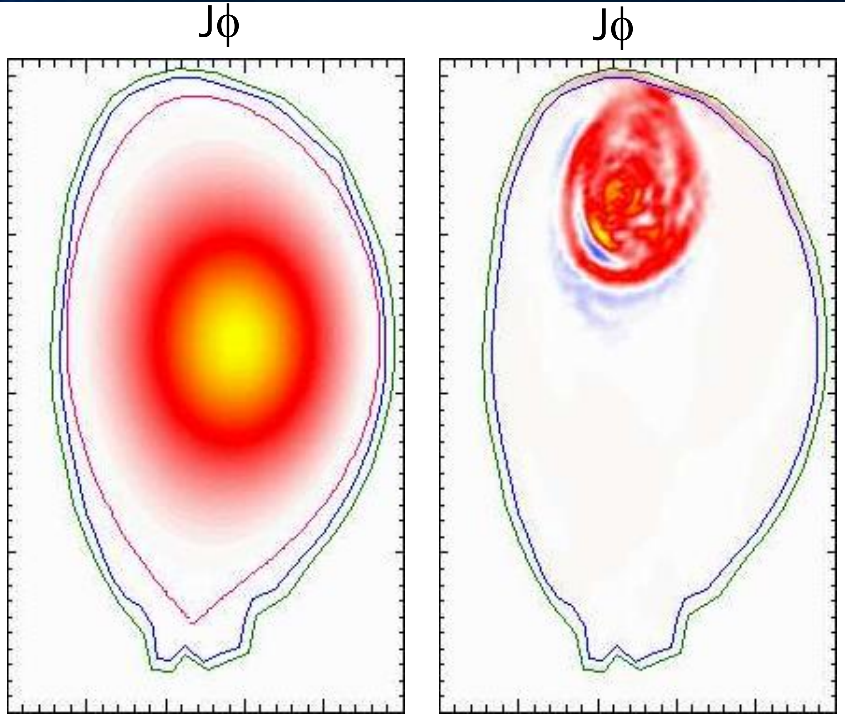

t = 0.0 ms   t = 2.2 ms

- Plasma drifts upward and scrapes off, reducing the edge safety factor q(a)

- Sideways force arises when q(a) < 1 and large (1,1) mode develops

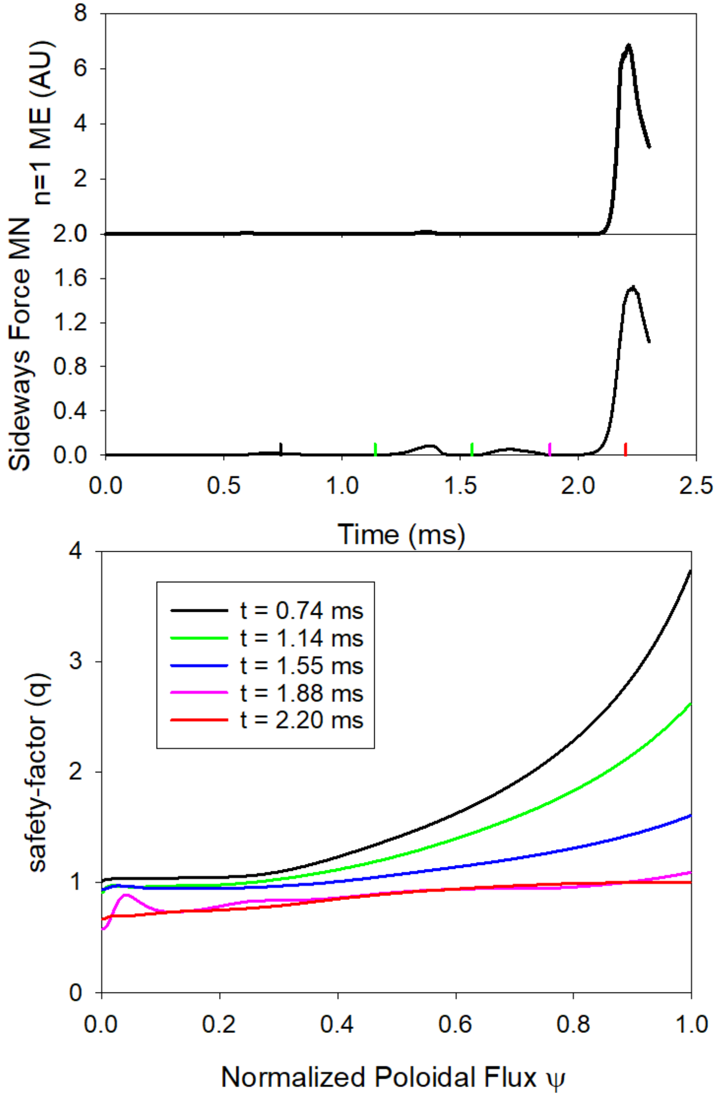

Strauss, IAEA, 2020

3D M3D-C¹ simulation of JET VDE shows origin and magnitude of sideways force

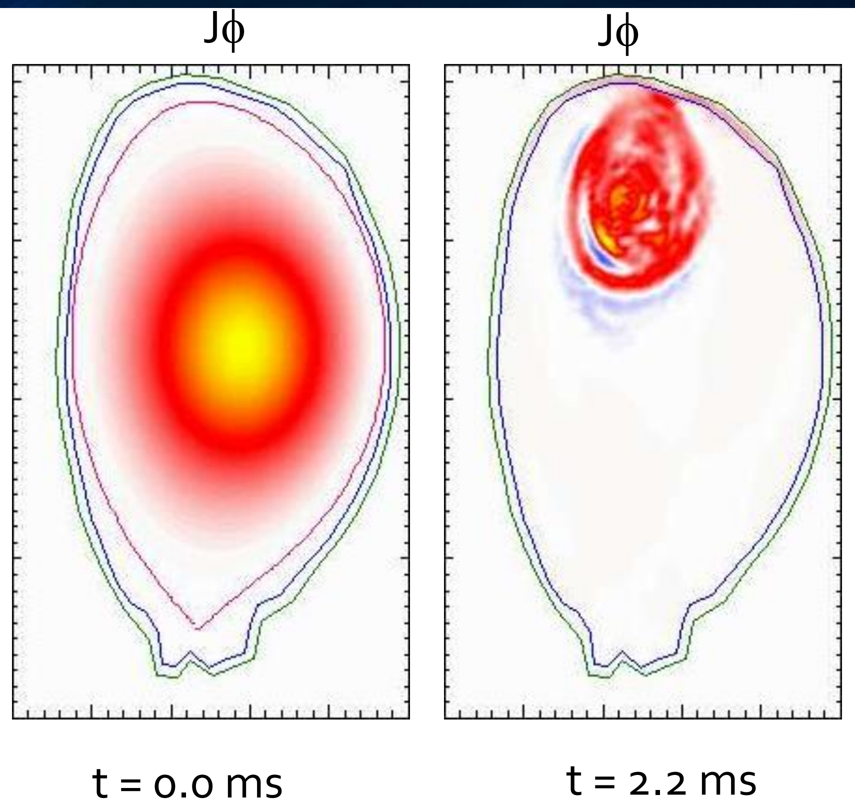

- Plasma drifts upward and scrapes off, reducing the edge safety factor q(a)
- Sideways force arises when q(a) < 1 and large (1,1) mode develops

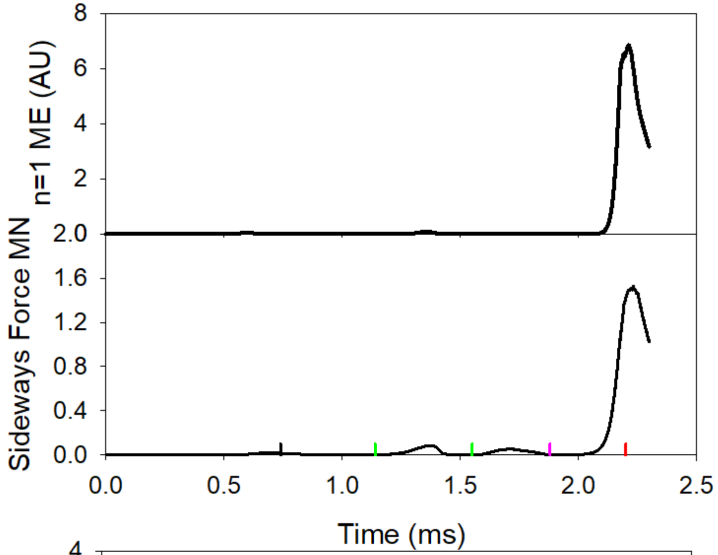

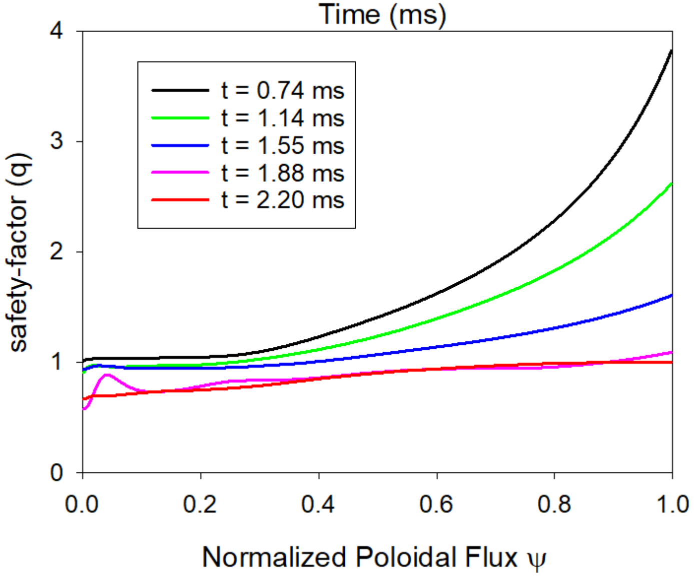

First self-consistent explanation of the origin of the horizontal force in a VDE

Strauss, IAEA, 2020

We have developed a comprehensive model of the ITER vessel and other conducting structures

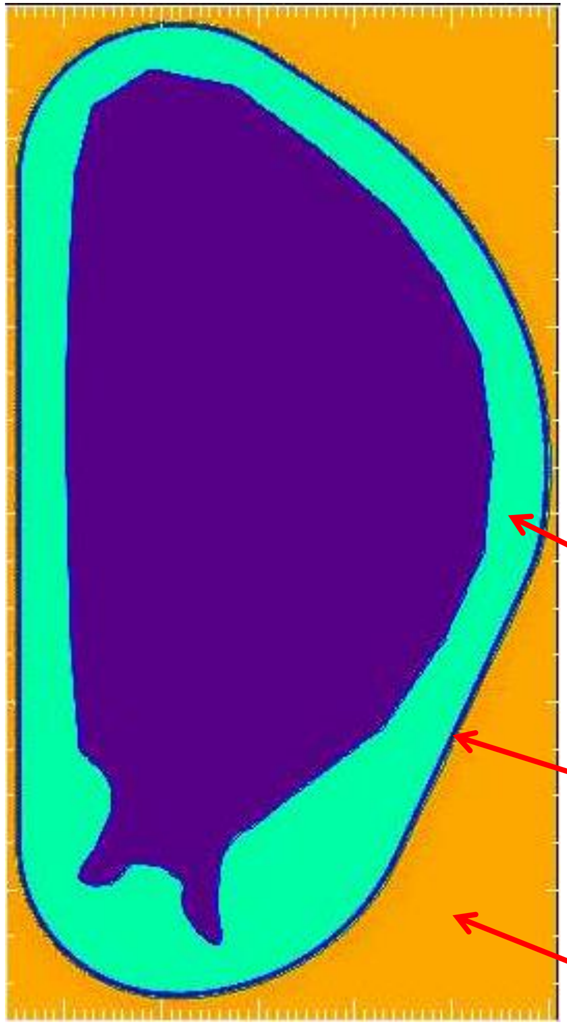

- The ITER conducting structures are complex : approximated by simpler model with realistic time-constants
- We presently have a 2-region ITER structure model with anisotropic resistivity to approximate actual ITER vessel including blanket modules
  - Conductor with high toroidal resistivity but low poloidal resistivity
  - 6-cm steel wall with low poloidal and toroidal resistivity
  - Vacuum region

- Very long vessel time constant > 200 ms
  - $\tau_W > 10^5\ \tau_A$

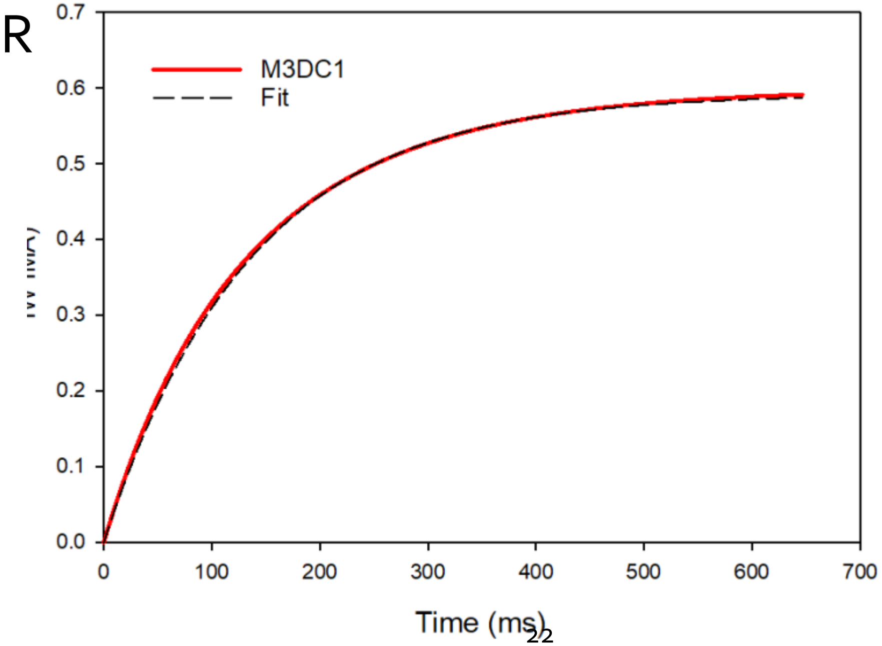

M3D-C¹ uses same triangular prism elements in all regions, plasma, structure, and vacuum

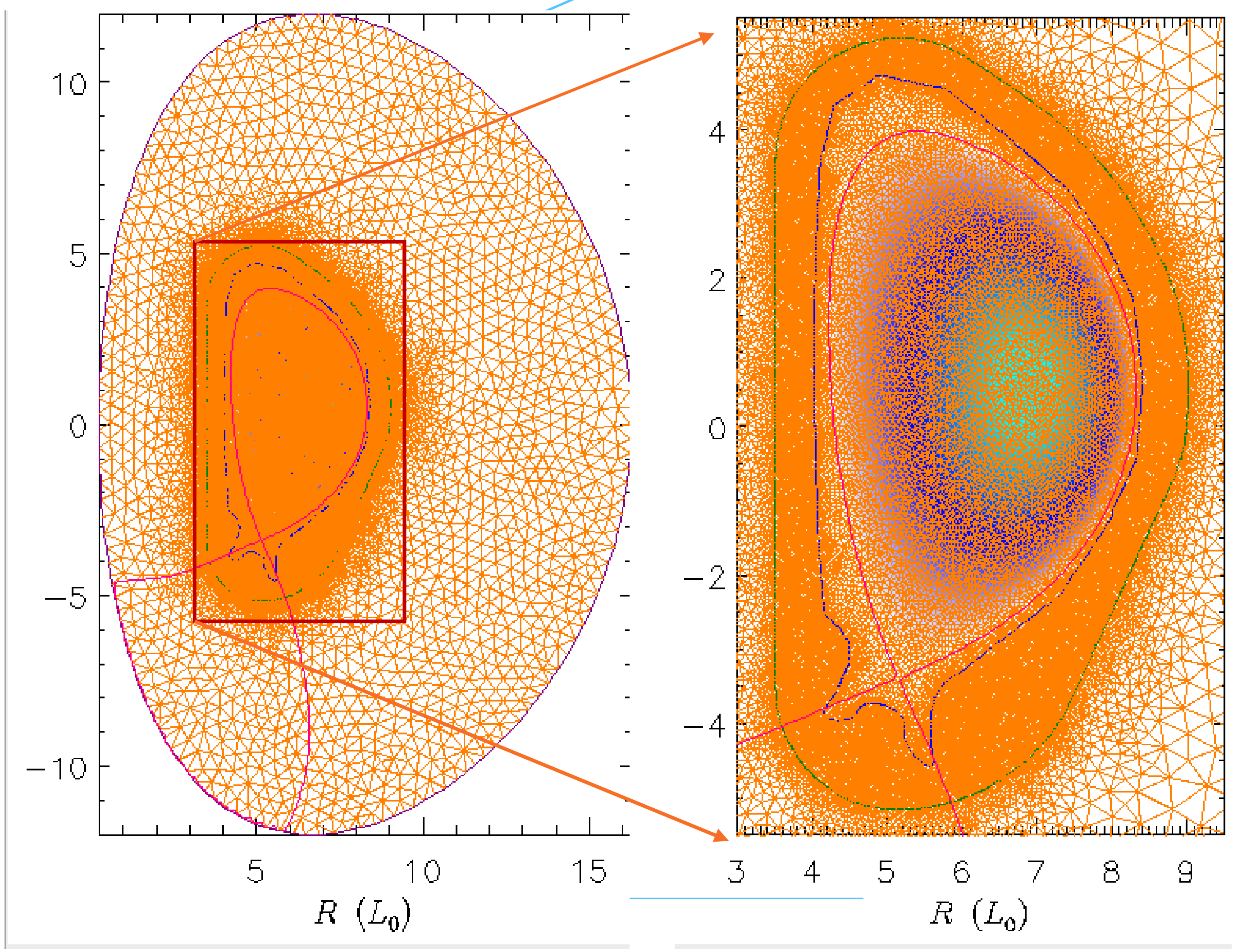

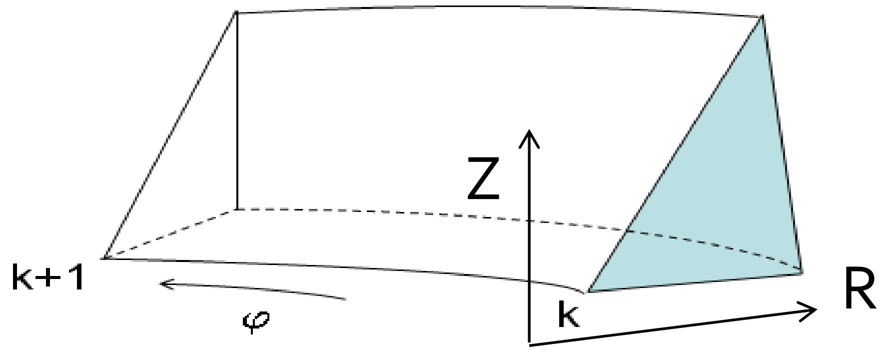

- Boundary conditions for the magnetic field are applied only at the outermost computational boundary

- Current is free to flow from the plasma to the conductors (halo currents) and the magnetic field will diffuse through the conductor

Typical 2D ITER M3D-C¹ VDE Simulation with new vessel model

Ψ@ t = 0
Diverted (t = 0)

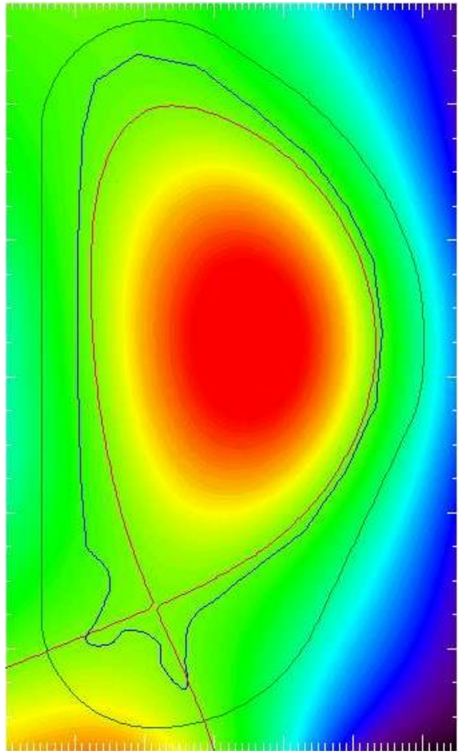

Ψ@ t = 64 ms
q(a) = 5 (t = 65 ms)

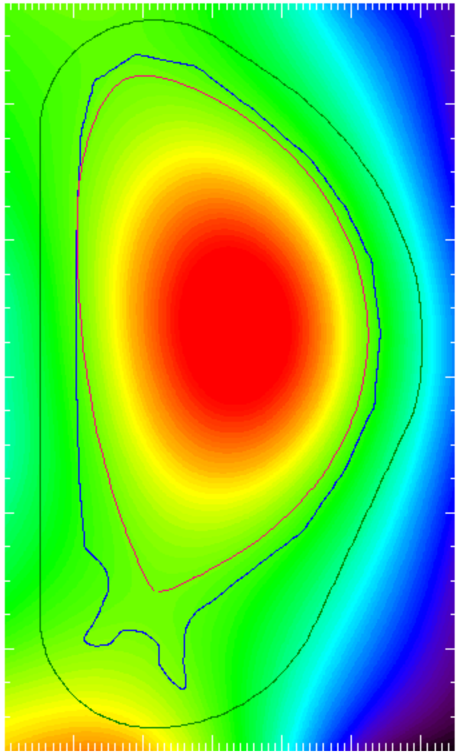

First becomes limited

Ψ@ t = 155 ms
q(a) = 2 (t = 152 ms)

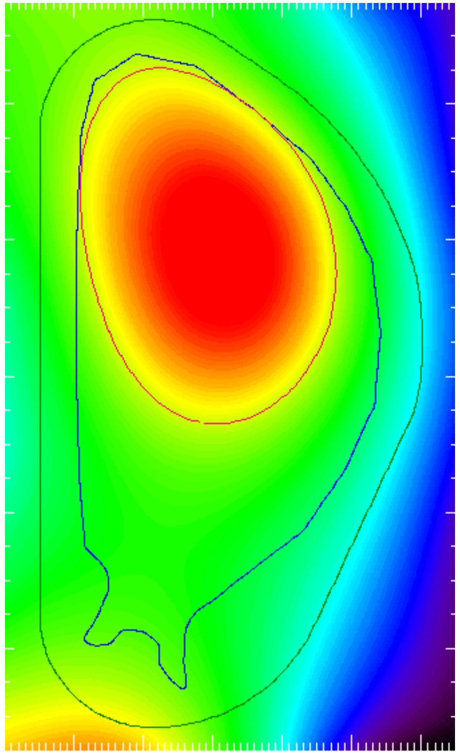

Start of Thermal Quench

Ψ@ t = 186 ms
q(a) = 1.1 (t = 184 ms)

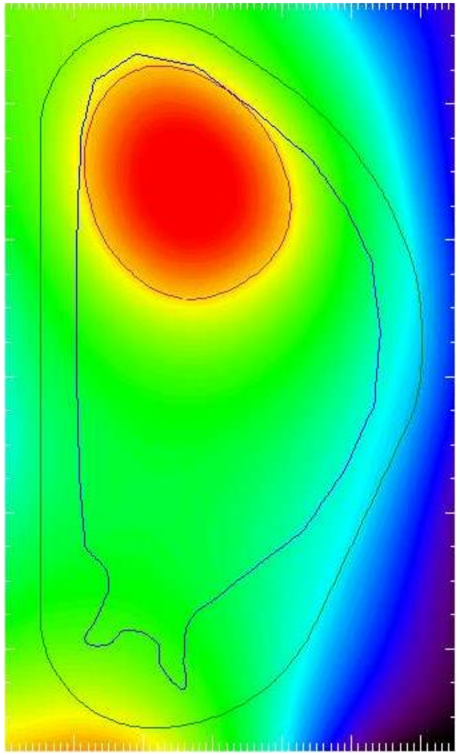

End of Calculation (when forces start to decrease)

Extensive 3D M3D-C¹ ITER simulations with new vessel model shows horizontal force much smaller than in JET !

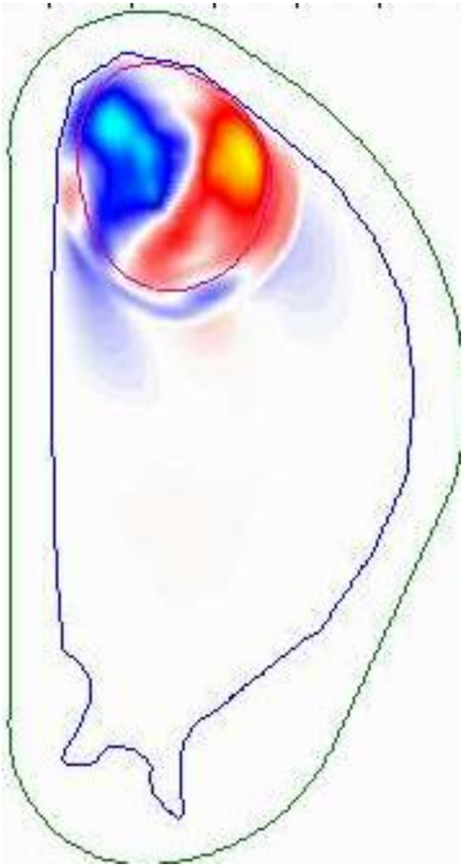

Max horizontal force in ITER less than 1 MN (~ 2 MN in JET)

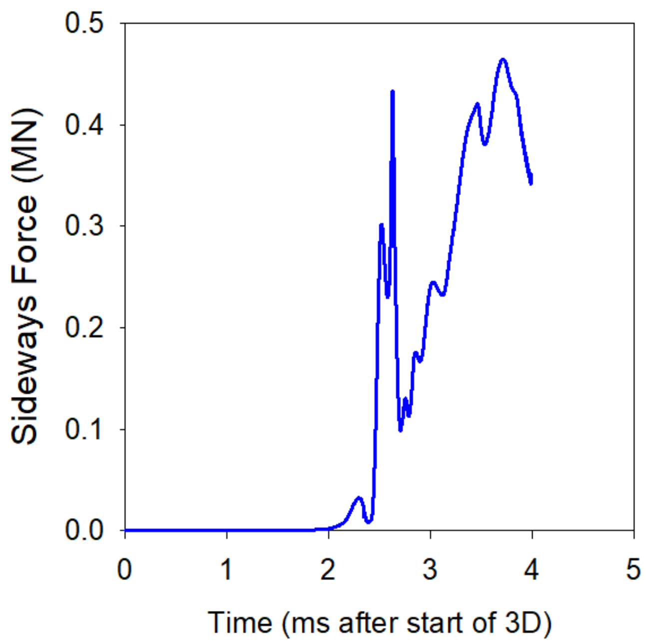

- The reason the force is so small is that the ITER vessel is such a good conductor that the scrape-off time is longer than the current quench time, so q(a) never falls below 1
- This is a striking (and controversial) result that is good news for ITER
- We are now repeating this run for a range of vessel resistivities to clarify the physics and solidify the conclusions. Great interest by ITER

Strauss, IAEA, 2020

Center for Tokamak Transient Simulations -- Outline

1. Code Descriptions and code benchmarks
2. Forces due to Vertical Displacement Events
3. Disruption Mitigation via Impurity Injections
4. Runaway Electrons interacting with MHD
5. Neoclassical Tearing Modes and Mode Locking
6. Sawteeth and Sawtooth-free discharges
7. Soft beta limits and disruption avoidance
8. List of talks at 2021 Theory and Simulation of Disruption Workshop
9. Publications
10. Summary
11. Future Plans

If a disruption is deemed imminent, it will be mitigated by the injection of a mm sized impurity pellet to radiate away the stored energy

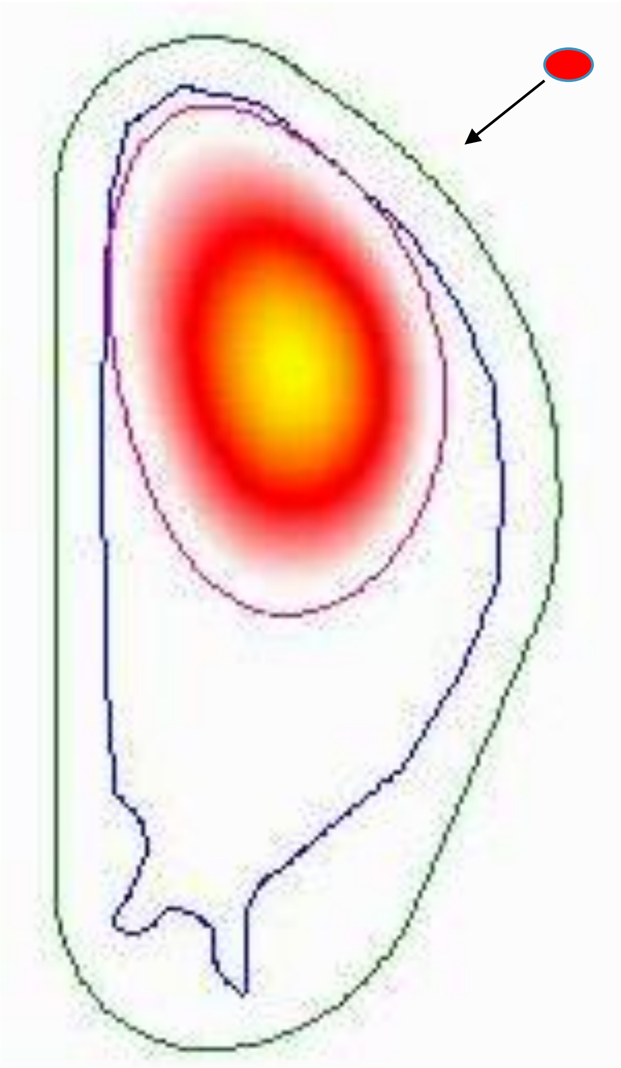

- Modeling this is is a multiscale problem, and we are pursuing two approaches

- The "standard" approach is to use an analytic model to describe the ablation of the pellet (and source of impurities) as a function of the plasma temperature and density

$$\dot{n} = f\left(T_e(t), n_e(t), \ldots\right)$$

- We are also pursuing a "2-code" approach where a separate code is computing the pellet ablation physics

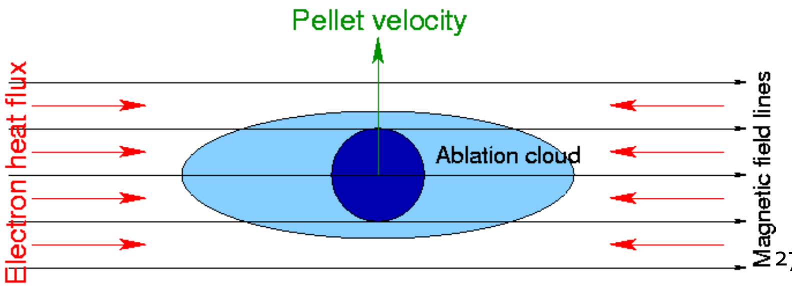

M3D-C¹ & NIMROD impurity-MHD modeling using the analytic ablation models have been successfully benchmarked[1]

- 2D, NL benchmark completed[1]
  - DIII-D plasma
  - Neon or argon injected on-axis
- Excellent agreement deep into nonlinear phase
  - Global quantities: P_{rad}, etc
  - Contours of T_e and J
- 3D, nonlinear benchmark in progress

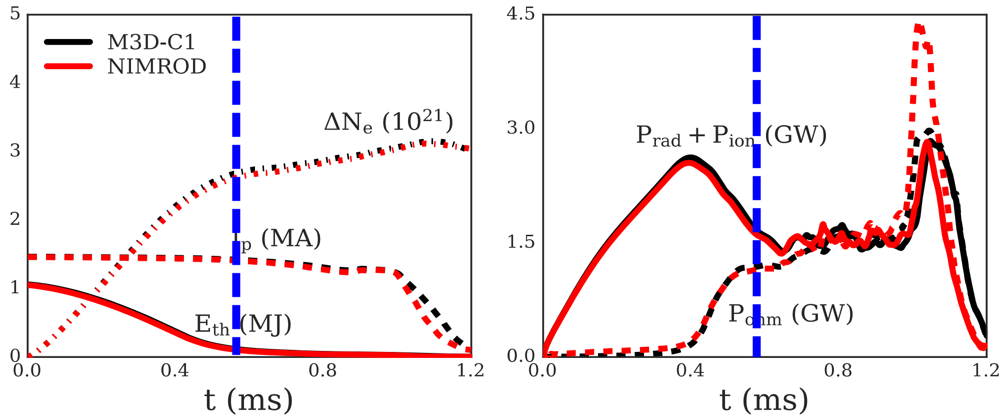

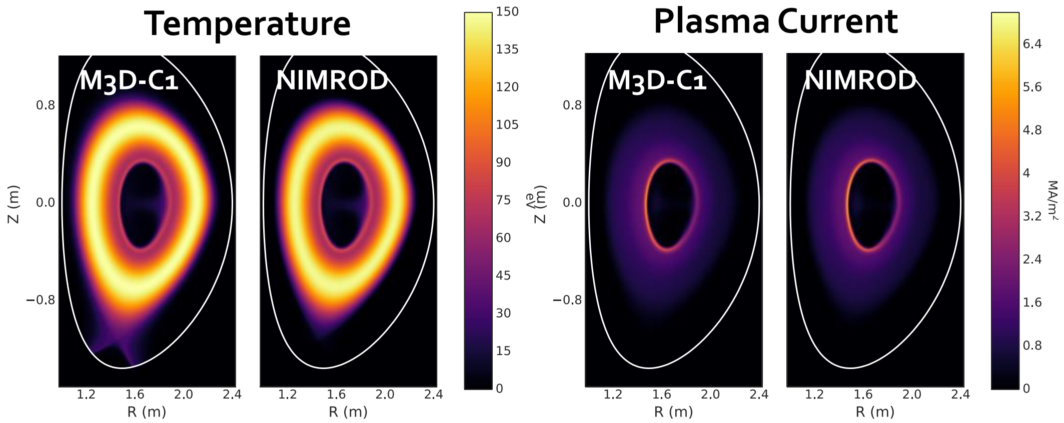

Lyons et al. PPCF 61, (2019).

Codes have been used to evaluate an electromagnetic pellet injector (EPI); There is a proposal to test on NSTX-U

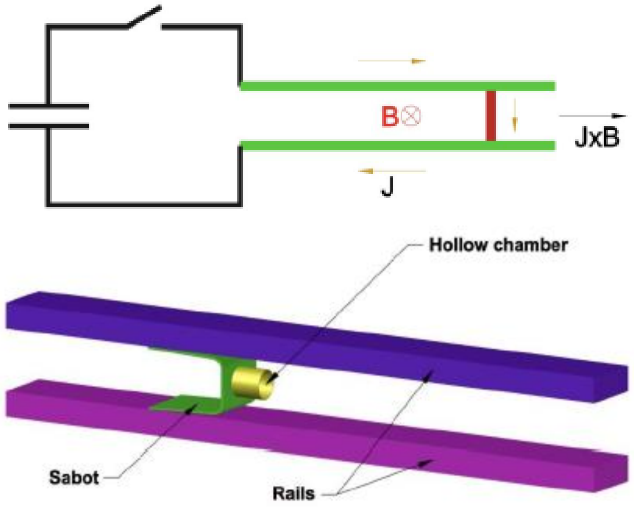

- Rail gun accelerates a sabot that contains 1 or more carbon pellets
- Very fast response time (2-3 ms) and speeds up to 1 km/s
- Analytic model of the carbon pellet ablation rate

Electron Temperature

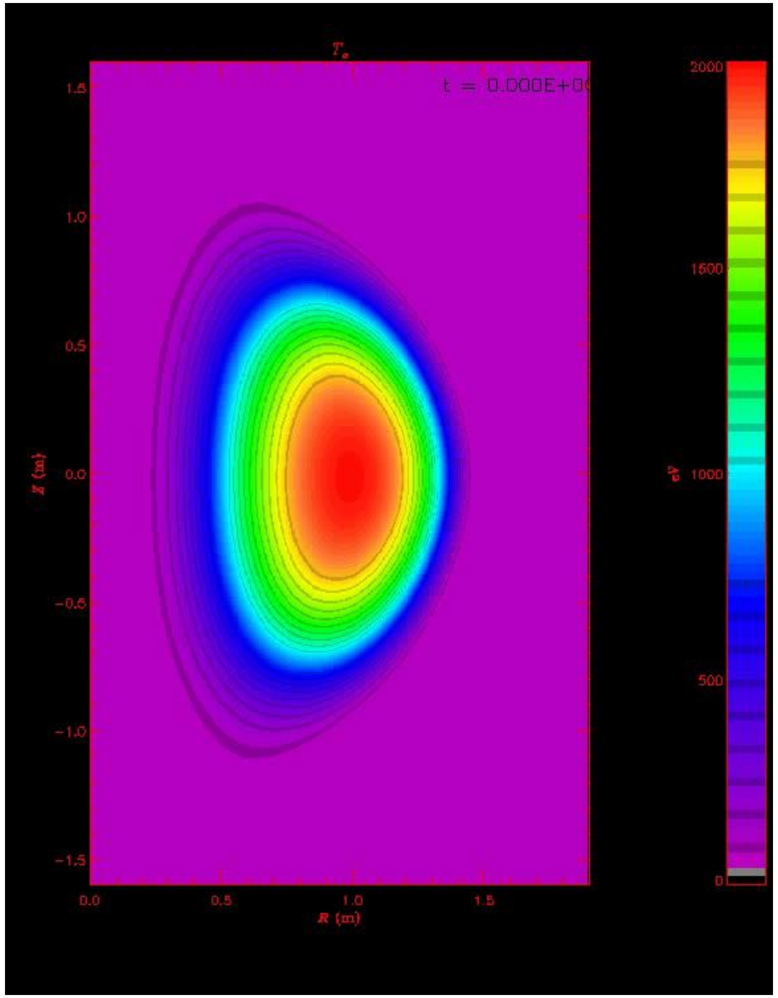

$Te(0) = 2$ keV

$n(0) = 2 \times 10^{19}$ m^{-3}

$I_P = 600$ kA

$\beta p = 0.73$

$li(3) = 0.6$

 Clauser, NF (2021)

Snapshots of EPI carbon pellet injected into NSTX-U show flux-surface breakup ahead of pellet

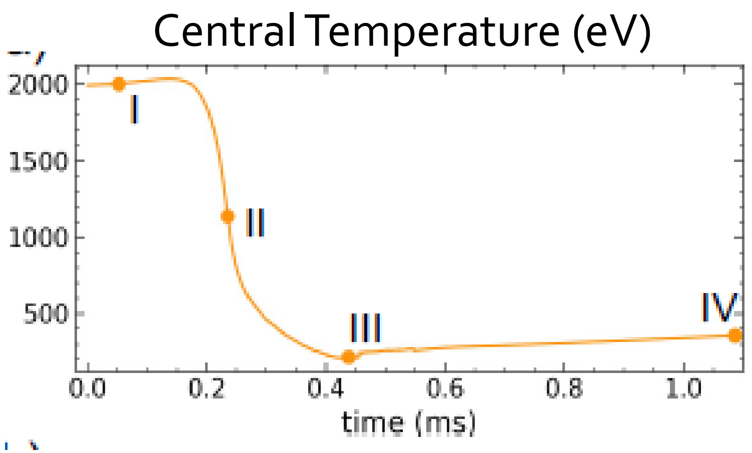

I - pellet enters from LFS

II – pellet excites MHD activity which breaks up surfaces ahead of pellet

III – when pellet reaches center, temperature profiles is hollow

IV – pellet exits now cooled plasma

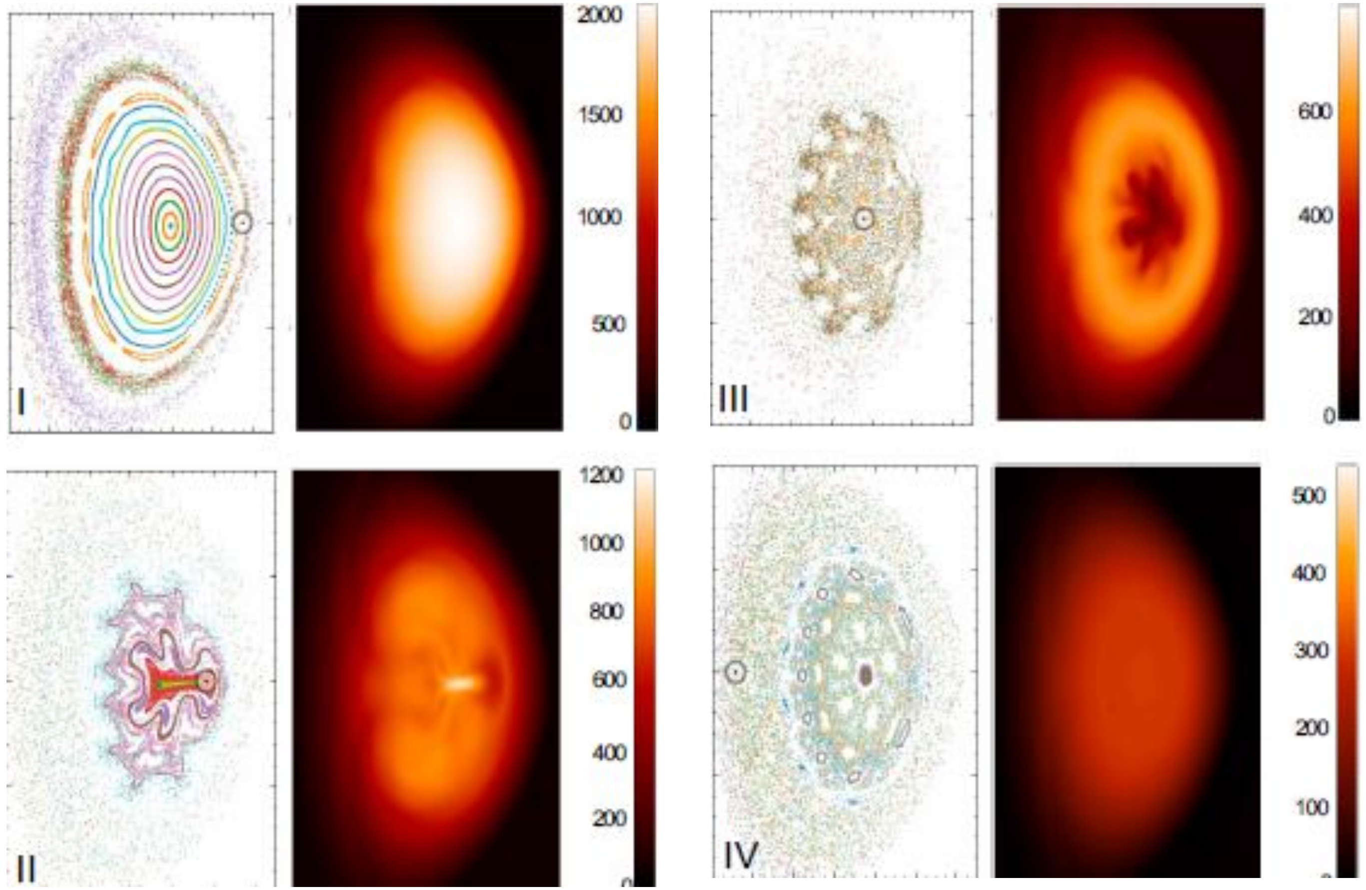

Clauser, NF (2021

NIMROD has been used to support the experimental comparison of Dual SPI injector on DIII-D with Single injector

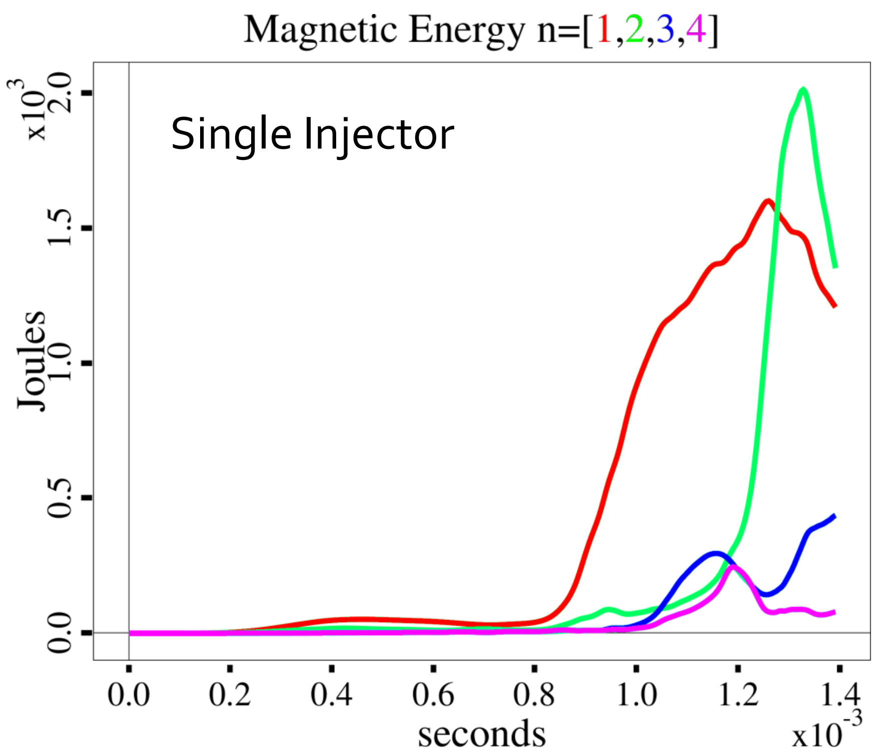

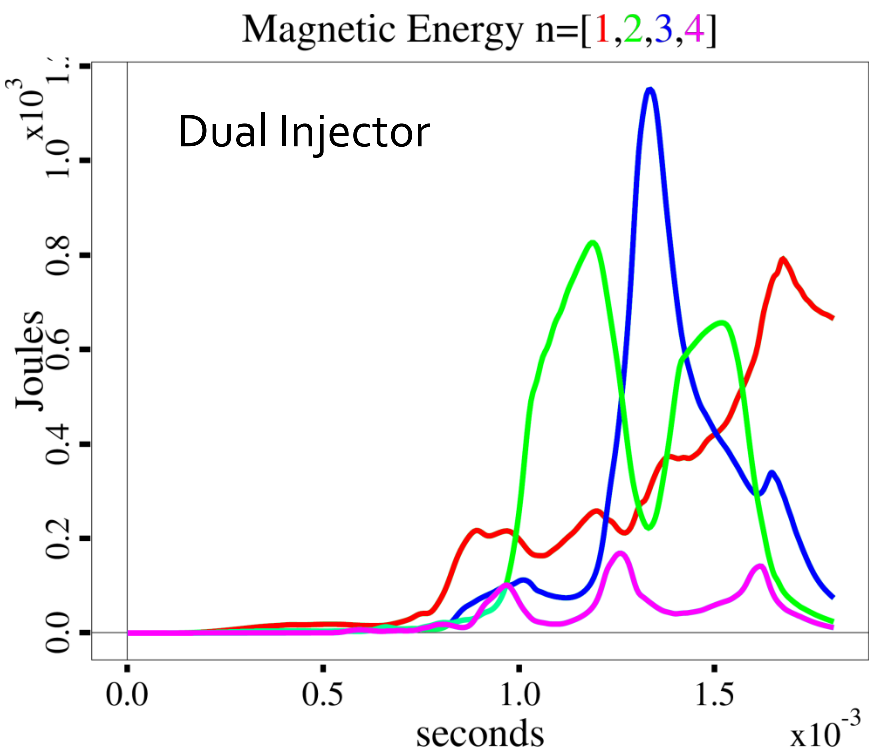

Dual injector (on right, separated by 120°) shows less energy in low-n MHD modes, which leads to a more benign thermal quench

Same total impurity

Kim, NF (2019)

Animation of single upper injection showing Impurity Density, Temperatue and Radiation contours

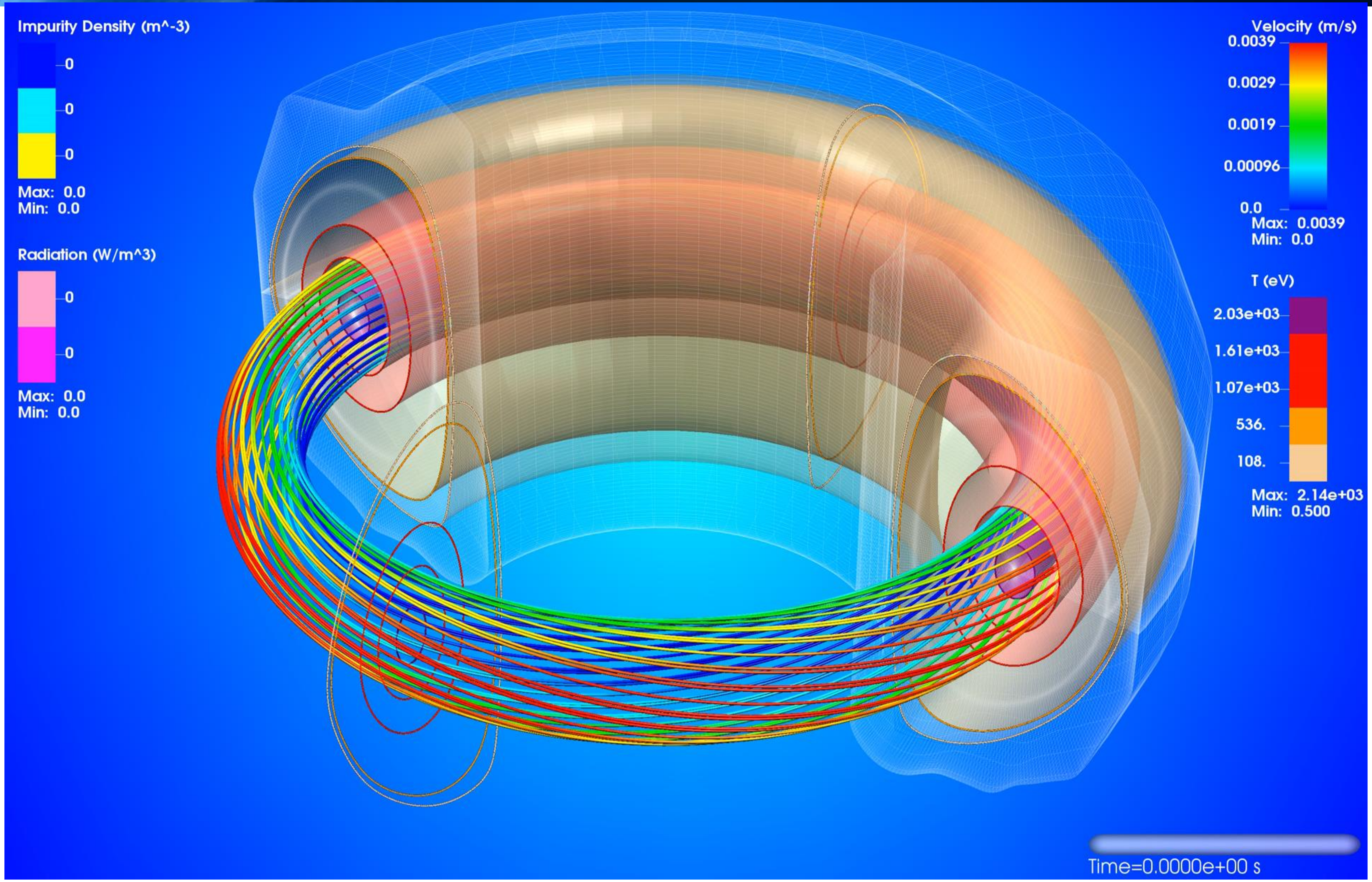

- the main contour shows the temperature.
- a single magnetic field line is included to help visual perspective.
- the pink contours are the radiation
- Radiation on can be seen to spread poloidally as the plume broadens
- the blue/aqua/yellow contours are impurity density.
- arrows indicate plasma flow on T~100eV surface.

C. Kim

Development of near-field codes for pellet ablation

Two codes were developed for calculating pellet ablation in the local approximation

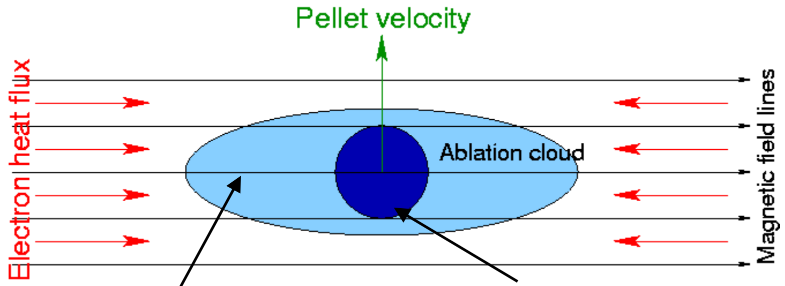

- Phase transition (ablation model) for pellet surface

- Low magnetic RE MHD equations
- Kinetic model for the electron heating
- EOS with atomic processes
- Radiation
- ∇B drift model for ablated material
- Pellet cloud charging models

Lagrangian Particle code (LP)

- Highly adaptive 3D particle code, massively parallel
- Lagrangian treatment of ablation material
- Supports large number of SPI fragments in 3D
- Imports far-field Te, ne, B from M3D-C[1]/NIMROD

FronTier code

- Legacy Hybrid Lagrangian-Eulerian with interface tracking
- Single pellet, 2D axisymmetric
- Played important role in initial verification of LP code

LP code computes the shielding length of the ablation cloud self-consistently as due to the grad-B drift

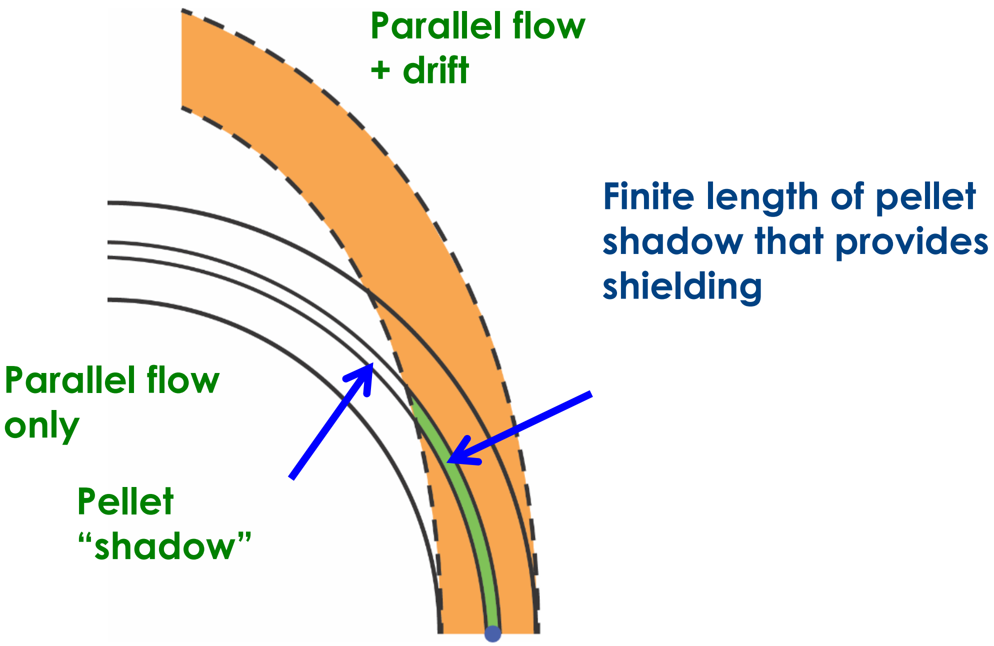

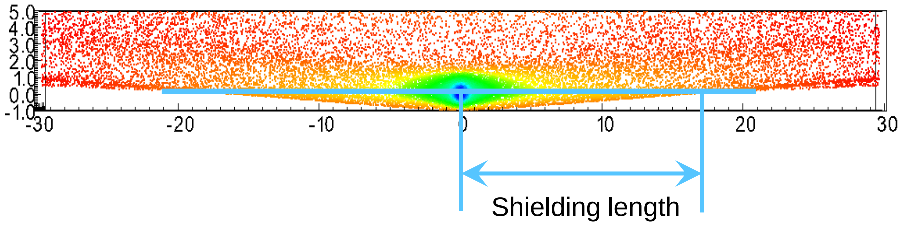

- The ablated material flows along the field line, but also grad-B drifts across the field
- This results in a finite shielding length (which strongly affects the ablation rate)
- The results of these calculations are used to improve the analytic ablation models and project them to ITER

R. Samulyak

Main accomplishments of “local” pellet modeling

I. Verification, code comparison, and studies of scaling laws

$$G \sim T_{e\infty}^{\frac{5}{3}} n_{e\infty}^{\frac{1}{3}} r_p^{\frac{4}{3}}$$

II. Comprehensive study of pellet ablation rates in magnetic fields with grad-B drift

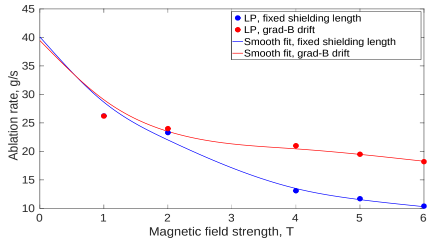

III. Initial coupled simulations with LP and M3D-C¹ code

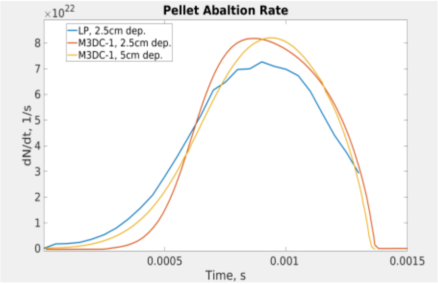

IV. Simulation of Shattered Pellet Injection into a runaway electron beam in ITER

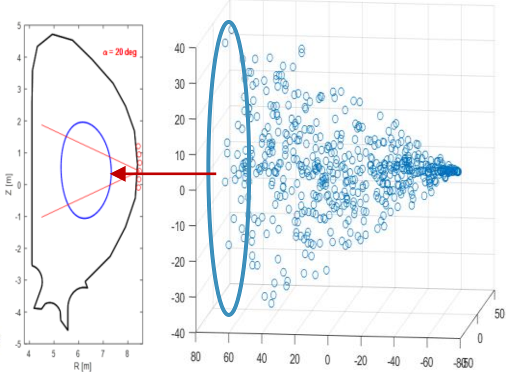

V. Optimization of massively parallel LP code using P4EST (parallel forest of K-trees)

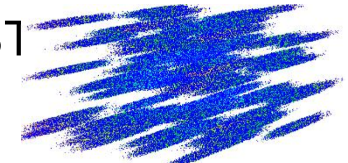

R. Samulyak

Center for Tokamak Transient Simulations -- Outline

1. Code Descriptions and code benchmarks
2. Forces due to Vertical Displacement Events
3. Disruption Mitigation via Impurity Injections
4. Runaway Electrons interacting with MHD
5. Neoclassical Tearing Modes and Mode Locking
6. Sawteeth and Sawtooth-free discharges
7. Soft beta limits and disruption avoidance
8. List of talks at 2021 Theory and Simulation of Disruption Workshop
9. Publications
10. Summary
11. Future Plans

Integrated modeling of Runaway Electrons (RE) with MHD

- New fluid runaway electron modules for both M3D-C¹ and NIMROD have been developed and are now being applied.
  - RE generation mechanisms (Dreicer, avalanche) are included.
- NIMROD has implemented a least-squares finite element evolution equation for the runaways with a nonlinear iteration to converge the magnetic advance
- M3D-C¹ has both a theta-implicit fluid advance and an advance based on the method of characteristics
- A collaboration between PPPL, GA, UW, and ORNL is initialized to couple both M3D-C¹ and NIMROD with KORC to model runaway electron diffusion and its back reaction to MHD instabilities

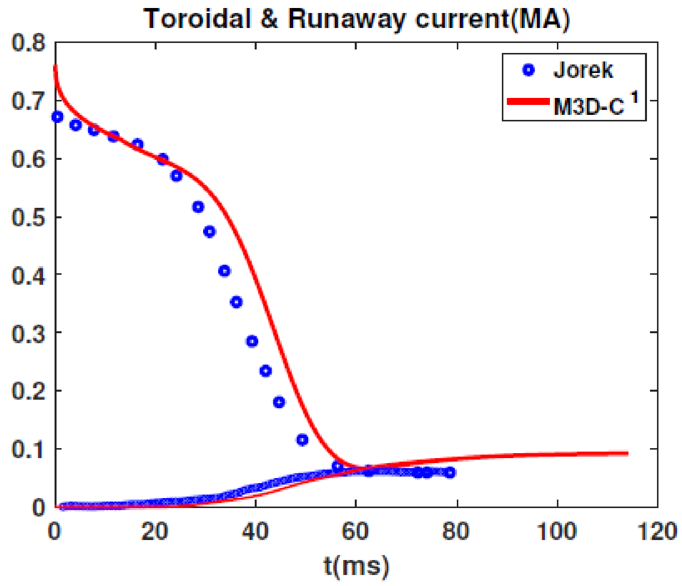

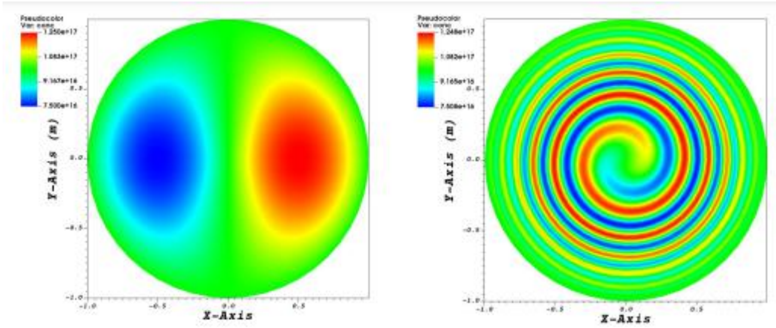

KORC: Highly scalable PIC RE code using GPUs (ORNL)

C. Liu, C. Zhao, B. Cornille, G. Wang, A. Sainterme,

Modeling of Runaway loss due to MHD instabilities (motivated by a similar experiment on DIII-D)

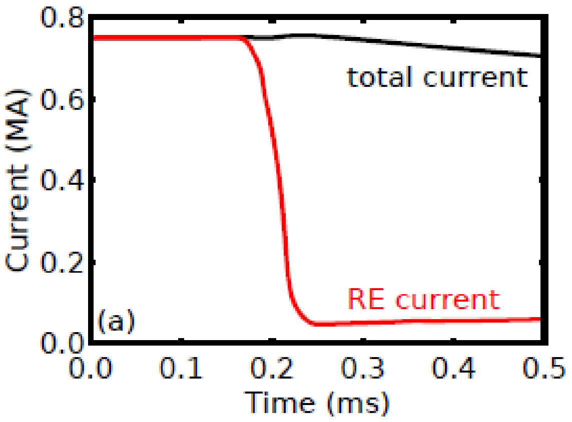

- A runaway discharge is intentionally scraped off to lower the edge q.
- By lowering the edge q you can excite a (2,1) instability that causes the runaways to get lost to the open field lines
- The current is then transferred to the bulk electrons….also seen in experiment

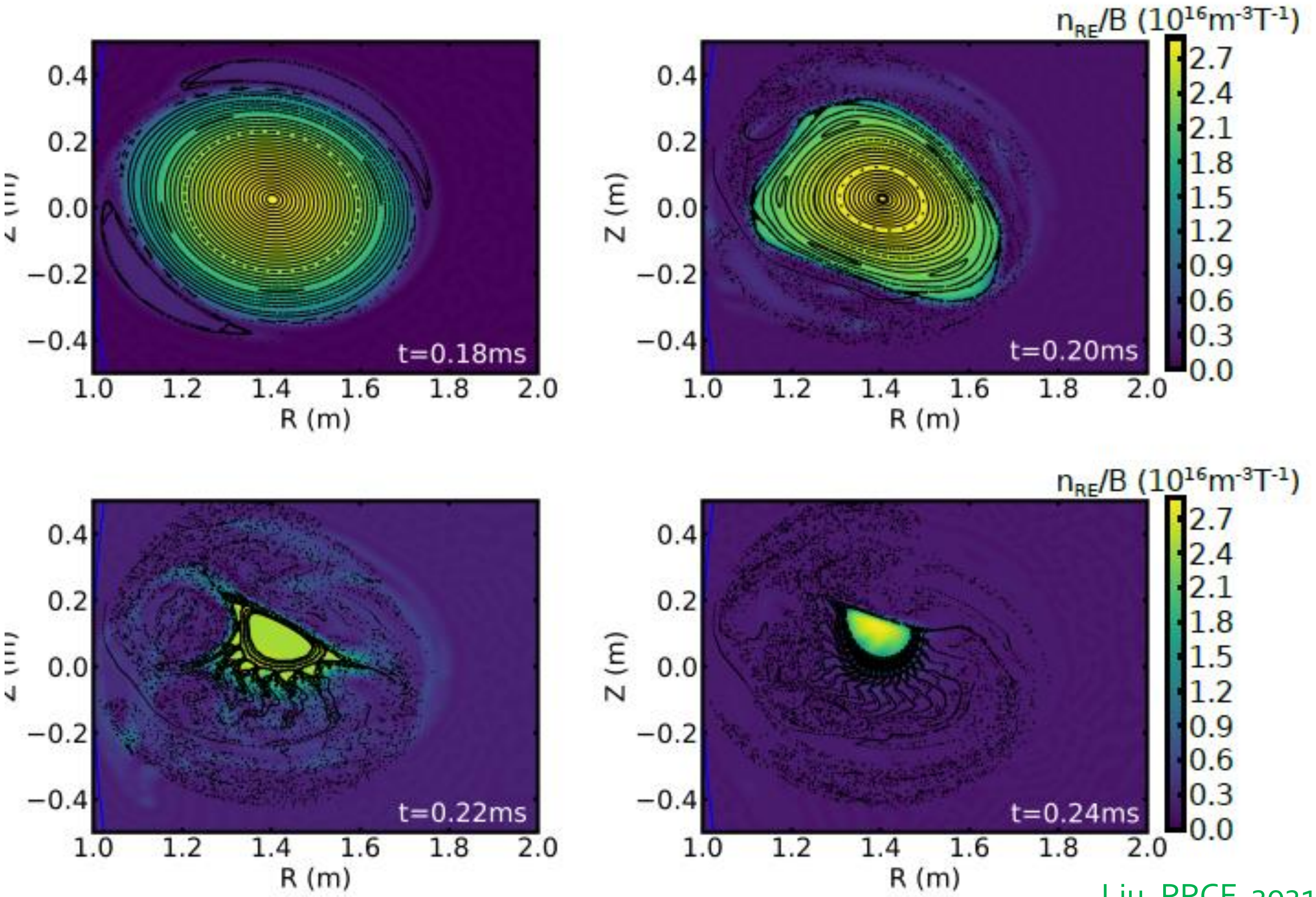

Liu, PPCF, 2021

Center for Tokamak Transient Simulations -- Outline

1. Code Descriptions and code benchmarks
2. Forces due to Vertical Displacement Events
3. Disruption Mitigation via Impurity Injections
4. Runaway Electrons interacting with MHD
5. Neoclassical Tearing Modes and Mode Locking
6. Sawteeth and Sawtooth-free discharges
7. Soft beta limits and disruption avoidance
8. List of talks at 2021 Theory and Simulation of Disruption Workshop
9. Publications
10. Summary
11. Future Plans

Neocclassical Tearing Modes (NTM) and Mode Locking

- Neoclassical tearing modes are the leading physics cause of disruption
- Three phases: seeding → locking → disruption
- Important details not yet understood:
  - Why do some transients seed NTMs but not others
  - How do locked NTMs trigger the thermal quench
- The NIMROD code has been extended to include heuristic closures for modeling NTMs
  - Immediate goal is to model a DIII-D discharge where an ELM at 3396 ms triggers a 2/1 NTM which grows to large amplitude and locks

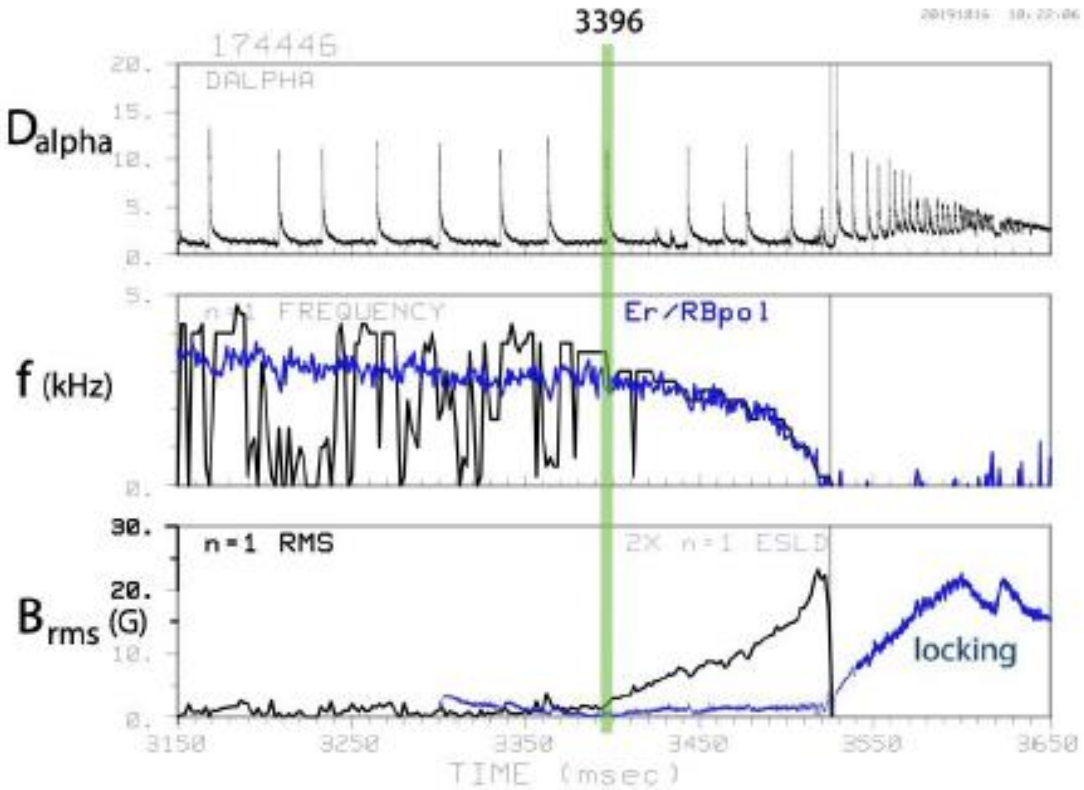

E. Howell, J. King, S. Kruger

Multiple phases of 2/1 mode following seed

- Initial slow growth phase now understood as complex linear and nonlinear interactions involving multiple toroidal modes n=1-6

- Later in time, the fast-growth phase is primarily n=1, and is well described by the Modified Rutherford Equation

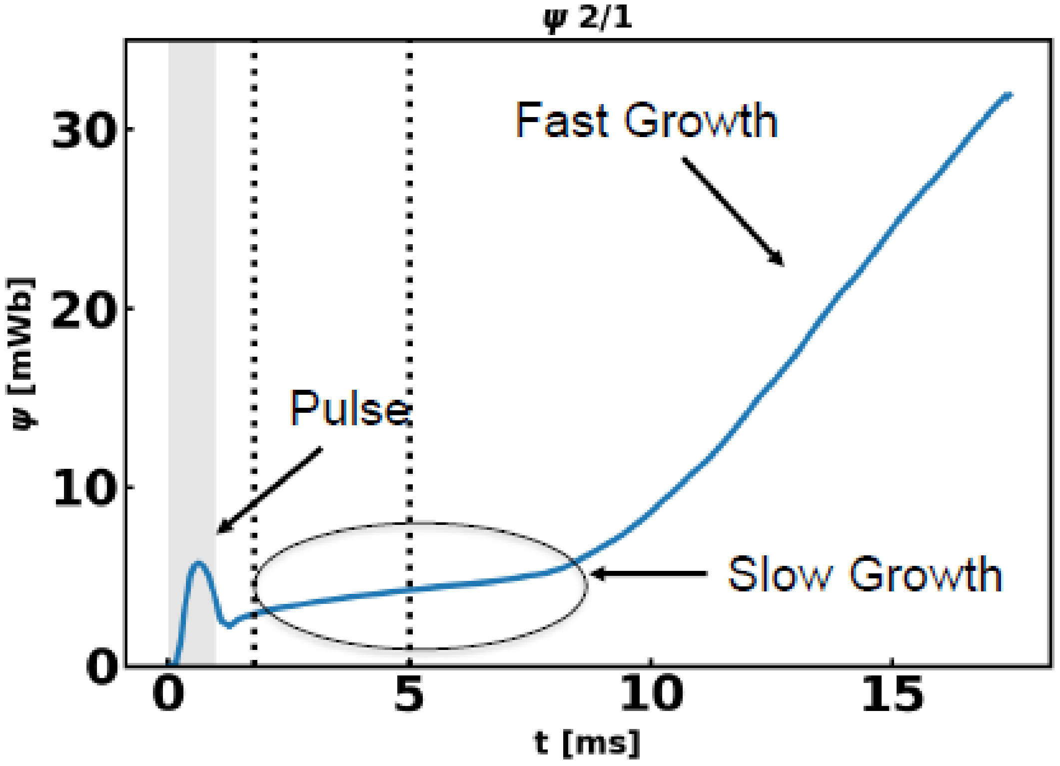

E. Howell, J. King, S. Kruger

A continuum kinetic model is being developed to replace the heuristic model now in NIMROD

- The total distribution function is represented as the sum of two parts: $$f(\mathbf{x},\mathbf{v},t) = f^{M}(\mathbf{x},\mathbf{v},t) + F(\mathbf{x},\mathbf{v},t)$$

Maxwellian from the NIMROD n_e, T_e, etc

Solve with kinetic equation using FE

- Algorithms are being tested for computing *F* efficiently and coupling it to NIMROD
- Several preconditioners are being evaluated for the implicit *F* equation
- Improvements have also been made in the evaluation of the Coulomb collision operator

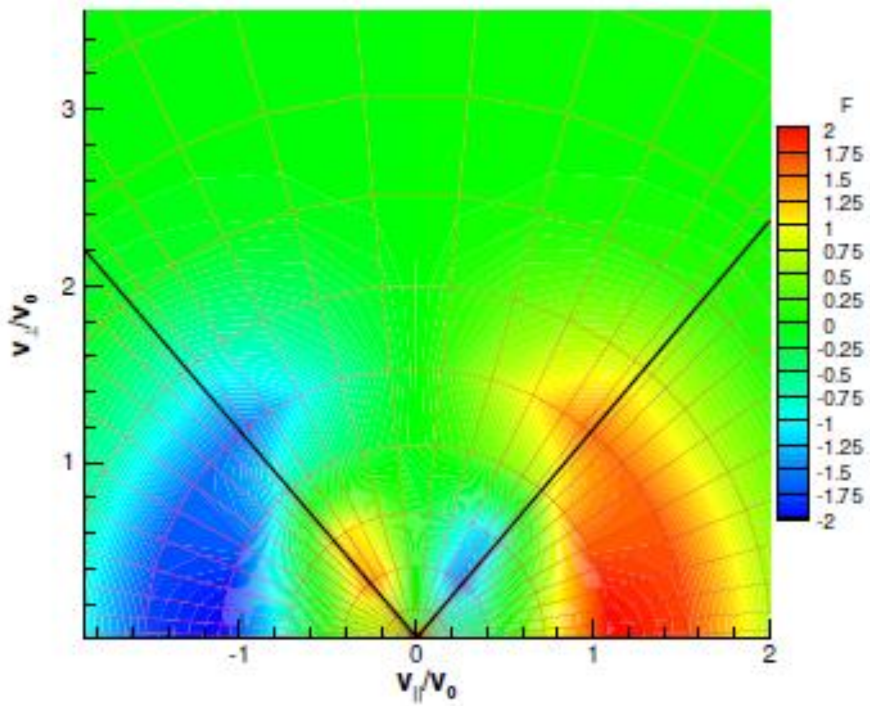

- Finite elements in velocity space use Gauss-Lobatto_Legendre elements to give extra resolution to trapped-passing boundary

E. Held, J. Ji, A. Spenser, T. Taylor, T. Markham, H. Lee, B. Adair

Center for Tokamak Transient Simulations -- Outline

1. Code Descriptions and code benchmarks
2. Forces due to Vertical Displacement Events
3. Disruption Mitigation via Impurity Injections
4. Runaway Electrons interacting with MHD
5. Neoclassical Tearing Modes and Mode Locking
6. Sawteeth and Sawtooth-free discharges
7. Soft beta limits and disruption avoidance
8. List of talks at 2021 Theory and Simulation of Disruption Workshop
9. Publications
10. Summary
11. Future Plans

Sawteeth and Sawteeth-free discharges

- New explanation for sawtooth oscillations came from simulation results
- Saturated (1,1) interchange mode in center produces dynamo voltage which keeps q(0) ~ 1 with low magnetic shear
- Sudden drop in temperature comes from pressure driven instabilities causing region in center to become stochastic
- (2,2), (3,3), (4,4) ….etc modes with sudden onset – q-profile doesn’t change
- If pressure peaking is limited, discharge will not sawtooth → hybrid discharges

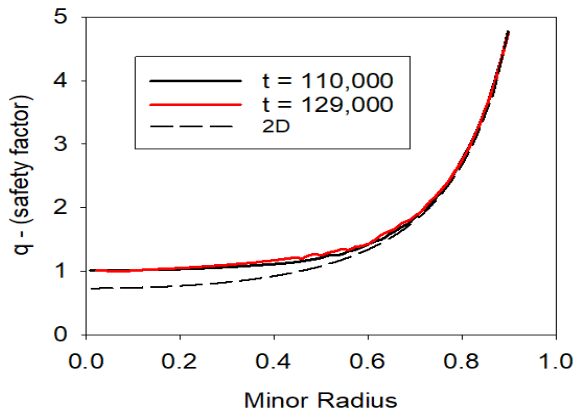

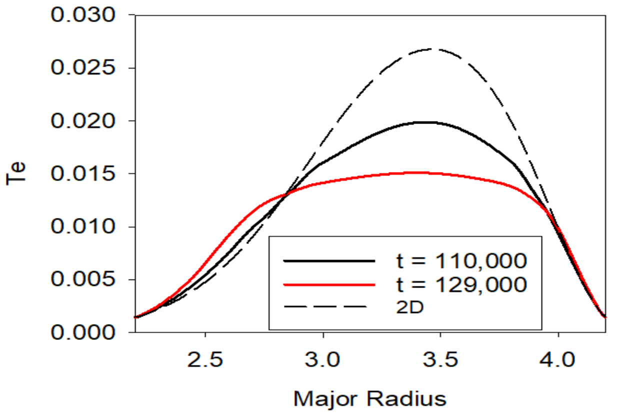

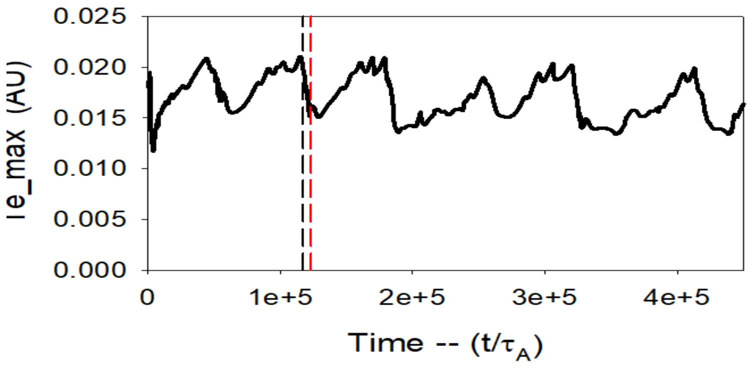

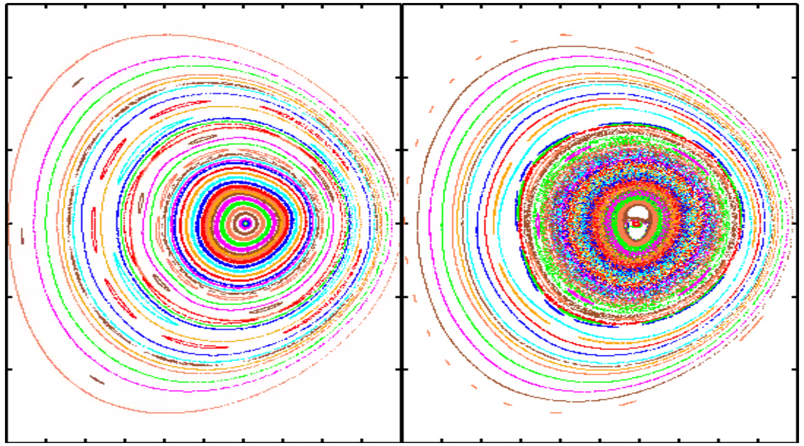

t = 110,000 t = 129,000

2020 Physics of Plasmas article has over 2500 downloads!

Center for Tokamak Transient Simulations -- Outline

1. Code Descriptions and code benchmarks
2. Forces due to Vertical Displacement Events
3. Disruption Mitigation via Impurity Injections
4. Runaway Electrons interacting with MHD
5. Neoclassical Tearing Modes and Mode Locking
6. Sawteeth and Sawtooth-free discharges
7. Soft beta limits and disruption avoidance
8. List of talks at 2021 Theory and Simulation of Disruption Workshop
9. Publications
10. Summary
11. Future Plans

400
400

Soft-beta limits in tokamaks

Poincare plots →

ΔTe →

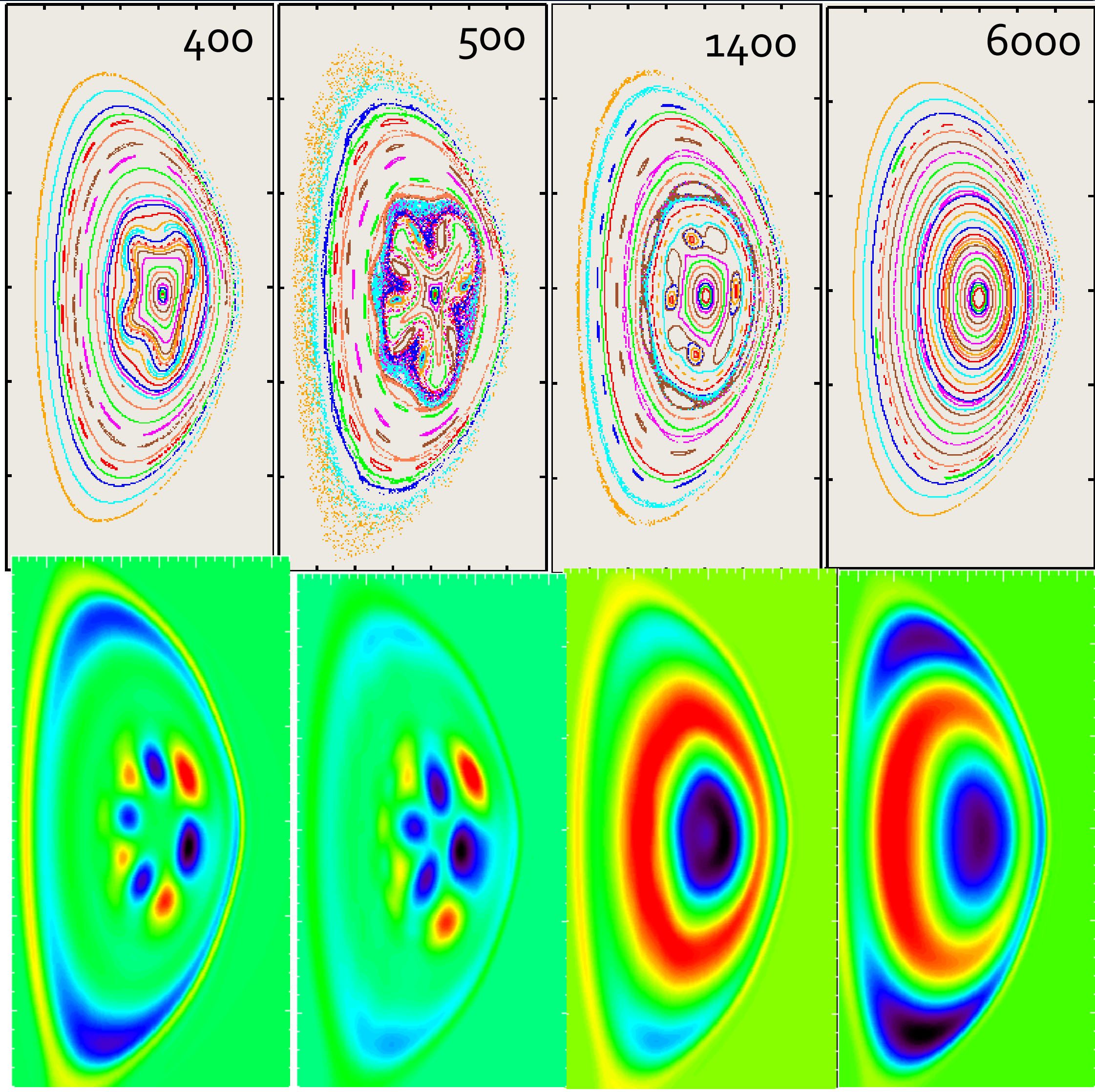

- Under certain conditions, heating a tokamak plasma to the β-limit and beyond, will not cause a disruption, but will drive localized instabilities that limit the β
- The magnetic surfaces first deform, become stochastic in a localized region, and then completely heal
- On the right we see a pure (4,3) mode goes unstable, first linear, then nonlinear, and it finally saturates and becomes axisymmetric again
- Our goal is to understand under what conditions this is likely to occur

Center for Tokamak Transient Simulations -- Outline

1. Code Descriptions and code benchmarks
2. Forces due to Vertical Displacement Events
3. Disruption Mitigation via Impurity Injections
4. Runaway Electrons interacting with MHD
5. Neoclassical Tearing Modes and Mode Locking
6. Sawteeth and Sawtooth-free discharges
7. Soft beta limits and disruption avoidance
8. List of talks at 2021 Theory and Simulation of Disruption Workshop
9. Publications
10. Summary
11. Future Plans

FY2021 “Theory and Simulation of Disruptions Workshop”

J. McClenaghan: MHD Modeling of SPI Injection in JET

V. Izzo: Dispersive Shell Pellet Modeling and Comparison with Experimental Trends

R. Samulyak: Simulation Study of Pellets and SPI Fragments Ablated by Thermal and Runaway Electrons

C. Sovinec: Findings from a Benchmark Study of 3D Vertical Displacement with JOREK, M3D-C^1 and NIMROD

H. Strauss: Thermal Quench in ITER Locked Mode Disruptons

C. Liu: Fast Wave Excited by Runaway Electrons in Disruptive Plasmas

C. Zhao: Simulation of Plateau Formation During Current Quench and MHD Instabilities with Runaway Electrons

E. Howell: Simulations of Neoclassical Tearing Modes Seeded via Transient Induced-Multimode Interaction

B. Lyons: Benchmarking Nonlinear Extended MHD Modeling of Disruption Mitigation

Related: Participation in ITPA Meetings

Several of our team are members of the ITPA on MHD, Disruptions, and Control and regularly attend meetings, make presentations, and serve on task forces

That group is presently preparing a Nuclear Fusion Review article "On the Path to Burning Plasma Operation"

S. Jardin has been asked to be the lead author for the Chapter: "Disruption Modeling"

Center for Tokamak Transient Simulations -- Outline

1. Code Descriptions and code benchmarks
2. Forces due to Vertical Displacement Events
3. Disruption Mitigation via Impurity Injections
4. Runaway Electrons interacting with MHD
5. Neoclassical Tearing Modes and Mode Locking
6. Sawteeth and Sawtooth-free discharges
7. Soft beta limits and disruption avoidance
8. List of talks at 2021 Theory and Simulation of Disruption Workshop
9. Publications
10. Summary
11. Future Plans

CTTS Publications 2021 (1 of 2)

F. Artola, C. Sovinec, S. Jardin, M. Hoelzl, I. Krebs and C. Clauser, “3D simulations of vertical displacement events in tokamaks: A benchmark of M3D-C1, NIMROD, and JOREK” , Phys. Plasmas **28** 052511 (2021)

M. Bosviel, P.B. Parks, and R. Samulyak, "Near-field models and simulations of pellet ablation in tokamaks ", Physics of Plasmas, **28,** 012506, (2021)

C. Clauser and S. Jardin, “ITER cold VDEs in the limit of a perfectly conducting first wall” Phys. Plasmas, **28**, 012511 (2021)

C. Clauser, S. Jardin, R. Raman, B. Lyons, N. Ferraro, “Modeling of carbon pellet disruption mitigation in an NSTX-U plasma”, to appear in Nuclear Fusion (2021)

N. Ding, Y. Liu, S. Williams, X.S. Li, ``A Message-Driven, Multi-GPU Parallel Sparse Triangular Solver'', Proc. of SIAM Conf. on Applied and Computational Discrete Algorithm (ACDA21), July 19-21, 2021.

J. R. Jepson, C. C. Hegna, E. D. Held, J. A. Spencer, and B. C. Lyons,” Benchmarking NIMROD Continuum Kinetic Formulations through the Steady-State Poloidal Flow”, Phys Plasmas **28**, 082503 (2021),

C. Liu, C. Zhao, S. Jardin, N. Ferraro, C. Paz-Soldan, Y. Liu, B. Lyons, “Self-consistent simulation of resistive kink instabilities with runaway electrons”, to appear in Plasma Physics and Controlled Fusion (2021)

CTTS Publications 2021 (2 of 2)

R. Samulyak, S. Yuan, N. Naitlho and P.B. Parks, "Lagrangian particle model for 3D simulation of pellets and SPI fragments in tokamaks", Nuclear Fusion, **61**, 046007, 2021.

H. Strauss and JET contributors, Effect of Resistive Wall on Thermal Quench in JET Disruptions, Phys. Plasmas **28**, 032501 (2021)

H. Strauss, Thermal quench in ITER disruptions, Phys. Plasmas **28** 072507 (2021)

A. Zafar, P. Zhu, A. Ali, S. Zeng, and H. Li, "Effects of helium massive gas injection level on disruption mitigation on EAST," Plasma Science and Technology **23**, 075103 (2021)

W. Zhang, S. C. Jardin, W. Ma, A. Kleiner, H. Zhang, "Nonlinear benchmarking between CLT and M3D-C1 for the 2/1 resistive tearing mode and the 1/1 resistive kink mode", Computer Physics Communications, **269**, 108134 (2021)

,

CTTS Publications 2020

K. J. Bunkers and C. R. Sovinec, “The influence of boundary and edge-plasma modeling in computations of axisymmetric vertical displacement,” Physics of Plasmas **27,** 112505 (2020)

N. Ding, S. Williams, Y. Liu, X.S. Li, ``Leveraging One-Sided Communication for Sparse Triangular Solvers'', Proc. of SIAM Conf. on Parallel Processing for Scientific Computing. Feb. 12-15, 2020, Seattle, pp. 93-105

S. Jardin, I. Krebs, N. Ferraro, “A New Explanation of the Sawtooth Phenomena in Tokamaks, Phys. Plasmas **27,** 032509 (2020)

J-Y. Ji, J. A. Spencer, and E. D. Held, “Exact irreducible moments of the Landau collision operator in the random-velocity moment expansion”, Plasma Research Express, **2**, (2020)

I Krebs, F J Artola, C R Sovinec, S C Jardin, K J Bunkers, M Hoelzl, N M Ferraro, Axisymmetric simulations of vertical displacements in tokamaks: A benchmark of M3D-C1, NIMROD, and JOREK, Phys. Plasmas **27** 022505 (2020)

C. Liu, C. Zhao, S. Jardin, A. Bhattacharjee, D. Brennan, N. Ferraro, “Structure and overstability of resistive modes with runaway electrons”, Phys. Plasmas **27**, 092507 (2020)

S. Munaretto, B. E. Chapman, B. S. Cornille, A. M. DuBois, K. J. McCollam, C. R. Sovinec, A. F. Almagri, and J. A. Goetz, “Generation and suppression of runaway electrons in MST tokamak plasmas,” Nucl. Fusion 60, 046024 (2020)

C. Zhao, C. Liu, S. C. Jardin, N. Ferraro, “Simulation of MHD instabilities with fluid runaway electron model in M3D-C1”, Nuclear Fusion 60 126017 (2020)

CTTS Publications 2019

S. Cheng, P. Zhu, D. Banerjee, X. Yan, and CFETR Physics Team, "Dominant two-fluid magnetohydrodynamic instabilities in CFETR upgrade phase-I scenario in presence of perfect conducting wall," Plasma Phys. Control. Fusion **61**, 045009 (2019).

C. Clauser, S. Jardin, N. Ferraro, Vertical forces during vertical displacement events in an ITER plasma and the role of halo currents, Nuclear Fusion **59** 126037 (2019)

C. C. Kim, Y. Liu, P. B. Parks, L. L. Lao, M. Lehnen, and A. Loarte, "Shattered pellet injection simulations with NIMROD", Physics of Plasmas, **26,** 042510, (2019)

B C Lyons, C C Kim, Y Q Liu, N M Ferraro, S C Jardin, J McClenaghan, P B Parks and L L Lao, "Axisymmetric benchmarks of impurity dynamics in extended-magnetohydrodynamic simulations", Plasma Physics and Controlled Fusion, **61**, 064001, (2019)

C. Sovinec and K. Bunkers, “Effects of asymmetries in computations of forced vertical displacement events”, Plasma Physics and Controlled Fusion **61** 024003 (2019)

CTTS Publications 2018

N.M. Ferraro, B.C. Lyons, C.C. Kim, Y.Q. Liu and S.C. Jardin, "3D magnetohydrodynamic modeling of fast thermal quenches due to impurities in tokamaks", Nuclear Fusion, **59**, 016001 (2018)

Pfefferle, D., Ferraro, N., Jardin, S.C., Krebs, I., “Modeling of NSTX hot Vertical Displacement Event using M3D-C1”, Phys. Plasmas **25** 056106 (2018)

R. Samulyak, X. Wang, H.-C. Chen, Lagrangian particle method for compressible fluid dynamics, Journal of Computational Physics, 362 (2018),

CS Team also part of group publications 2021

E. Suchyta, S. Klasky, N. Podhorszki, M. Wolf, A. Adesoji, C. S. Chang, J. Choi, P. E. Davis, J. Dominski, S. Ethier, I. Foster, K. Germaschewski, B. Geveci, K. A. Huck, C. Johnson, Q. Liu, J. Logan, K. Mehta, G. Merlo, S. V. Moore, T. Munson, M. Parashar, D. Pugmire, M. S. Shephard, P. Subedi, C. W. Smith, L. Wan, S. Zhang, “The Exascale Framework for High Fidelity coupled Simulations (EFFIS): Enabling Whole Device Modeling in Fusion Science”, *Int. J. High Performance Computing Applications*, p.10943420211019119, 2021, https://doi.org/10.1177/10943420211019119.

T. Kolev, P. Fischer, M. Min, J. Dongarra, J. Brown, V. Dobrev, T. Warburton, S. Tomov, M.S. Shephard, A. Adelfattah, V. Barra, N. Beams, J.-S. Camier, N. Chalmers, Y, Dudouit, A. Karlin, S. Kerkemeier, Y.-H. Lan, D. Medina, E. Merzari, A. Obabko, W. Pazner, T. Rathnayake, C.W. Smith, L. Spies, K. Swirydowicz, J. Thompson, A. Tomboulides, V. Tomov, “Efficient Exascale Discretizations”, *Int. J. High Performance Computing Applications*, 2021, https://doi.org/10.1177/10943420211020803

G. Diamond, C.W. Smith, C. Zhang, E. Yoon, M.S. Shephard, “PUMIPic: A mesh-based approach to unstructured mesh Particle-In-Cell on GPUs”, *J. Parallel and Distributed Computing*, 157:1-12, Nov. 2021, doi.org/10.1016/j.jpdc.2021.06.004.

J. Merson and M.S. Shephard, model-traits: Model attribute definitions for scientific simulations in C++, *J. Open Source Software*, 6(64), 1 3389, https://doi.org/10.21105/joss.03389

CS Team also part of group publications 2018,2019

G. Diamond, C.W. Smith, C. Zhang, E. Yoon, G. Perumpilly, O. Sahni and M.S. Shephard. "Towards Accelerated Unstructured Mesh Particle-in-Cell", Workshop on Latest Advances in Scalable Algorithms for Large-Scale Systems (ScalA '19). 2019.

C.W. Smith, B. Granzow, G. Diamond, D. Ibanez, O. Sahni, K.E. Jansen and M.S. Shephard, 2018. In-memory integration of existing software components for parallel adaptive unstructured mesh workflows. *Concurrency and Computation: Practice and Experience*, *30*(18), p.e4510.

G. Diamond, C.W. Smith, and M.S. Shephard. "Dynamic Load Balancing of Plasma and Flow Simulations", *Proceedings of the 8th Workshop on Latest Advances in Scalable Algorithms for Large-Scale Systems*. ACM, 2018.

Center for Tokamak Transient Simulations -- Outline

1. Code Descriptions and code benchmarks
2. Forces due to Vertical Displacement Events
3. Disruption Mitigation via Impurity Injections
4. Runaway Electrons interacting with MHD
5. Neoclassical Tearing Modes and Mode Locking
6. Sawteeth and Sawtooth-free discharges
7. Soft beta limits and disruption avoidance
8. List of talks at 2021 Theory and Simulation of Disruption Workshop
9. Publications
10. **Summary**
11. Future Plans

Summary

- Progress you have made during the first four years of your project
  - M3D-C1, NIMROD, LP code development, verification & validation, some projection to ITER

- Your plans for the last remaining year of your project
  - Incremental improvement: focus on validation and publications

- How the fusion side collaborated with the applied math / computer science side and the benefits from this collaboration
  - Mesh improvements, sparse matrix solves improvements, LC code development

- Looking ahead, what are the most critical but still unsolved problems in your field / topical area?
  - Continue code validation and projection to ITER parameters .. See next slide

Center for Tokamak Transient Simulations -- Outline

1. Code Descriptions and code benchmarks
2. Forces due to Vertical Displacement Events
3. Disruption Mitigation via Impurity Injections
4. Runaway Electrons interacting with MHD
5. Neoclassical Tearing Modes and Mode Locking
6. Sawteeth and Sawtooth-free discharges
7. Soft beta limits and disruption avoidance
8. List of talks at 2021 Theory and Simulation of Disruption Workshop
9. Publications
10. Summary
11. Future Plans

Center for Tokamak Transient Simulations Future Studies

1. Code Descriptions and code benchmarks: optimize codes for GPUs, improvements in physics models as required to improve validation results
2. Forces due to Vertical Displacement Events: Clarifications of reasons for small force, include ports in ITER vessel model, how best to reduce forces via mitigation
3. Disruption Mitigation via Impurity Injections: More validation, better neutrals model, global + local simulations, quantitative ITER simulations
4. Runaway Electrons interacting with MHD: Coupling with KORC (kinetic model), more validation, quantitative ITER simulations
5. Neoclassical Tearing Modes and Mode Locking: Continue validation, study physics of mode locking and Thermal Quench initiation, employ kinetic MHD model
6. Sawteeth and Sawtooth-free discharges: Extend simulations to higher S values, understand the role of plasma rotation, predictions for ITER
7. Soft beta limits and disruption avoidance: Validation. Identify trends

Extra vgs

Summary of 3D ITER VDE Simulations

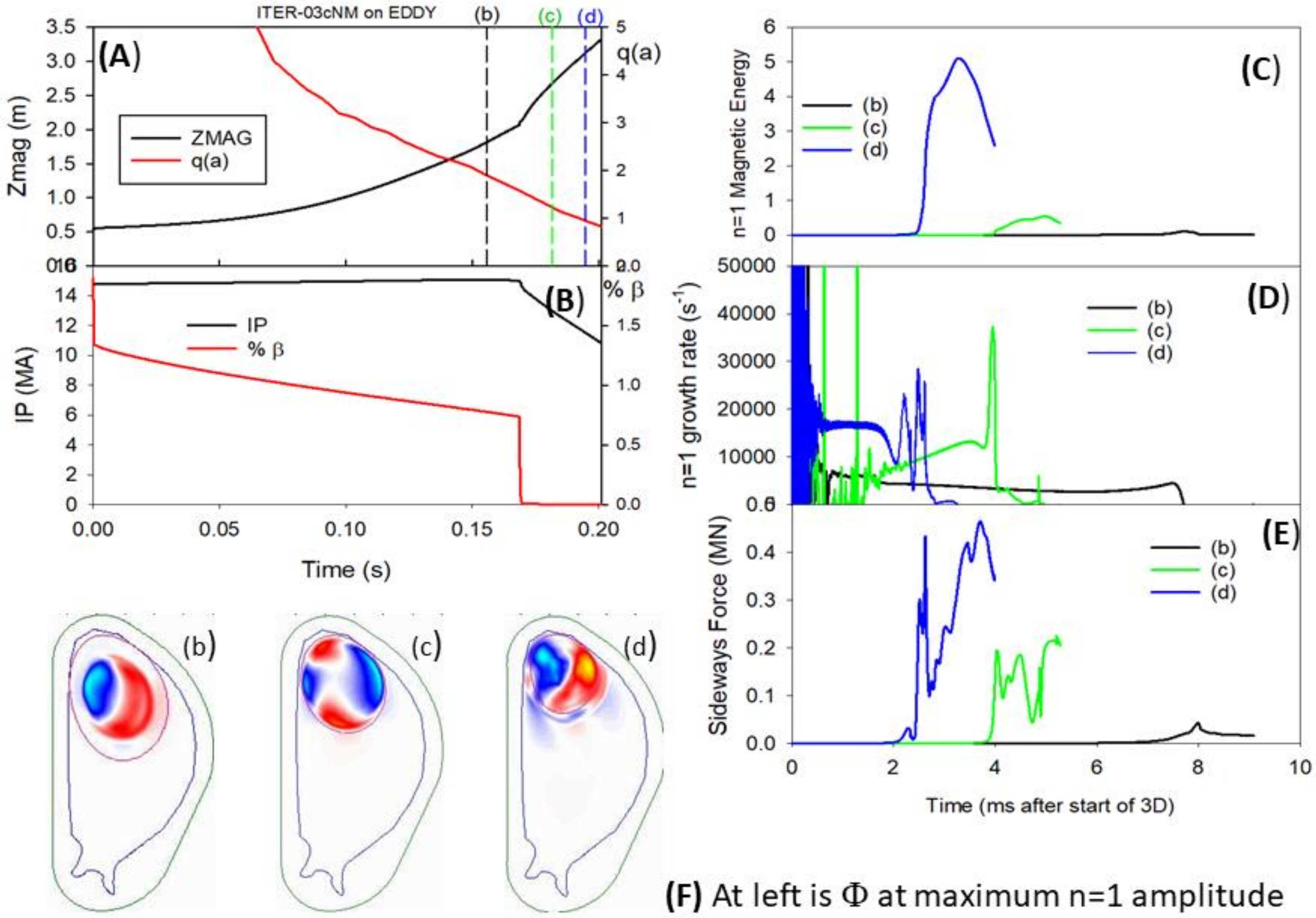

(F) At left is Φ at maximum n=1 amplitude

- Figs. (A), (B) show Z, q(a), I_P, β, from 2D simulation.
- 3D simulation begins at times
  - (b) q(a) = 1.7,
  - (c) q(a) = 1.2,
  - (d) q(a) = 0.9
- 3D results shown in (C)-(F)
- Max. horizontal force to date is less than 1 MN.

Why is the 3D horizontal force in ITER so small? (Less than that observed in JET)

To get a large horizontal force on the vessel, you need a large external (1,1) mode.
This will only occur if q(a) < 1 during the disruption.

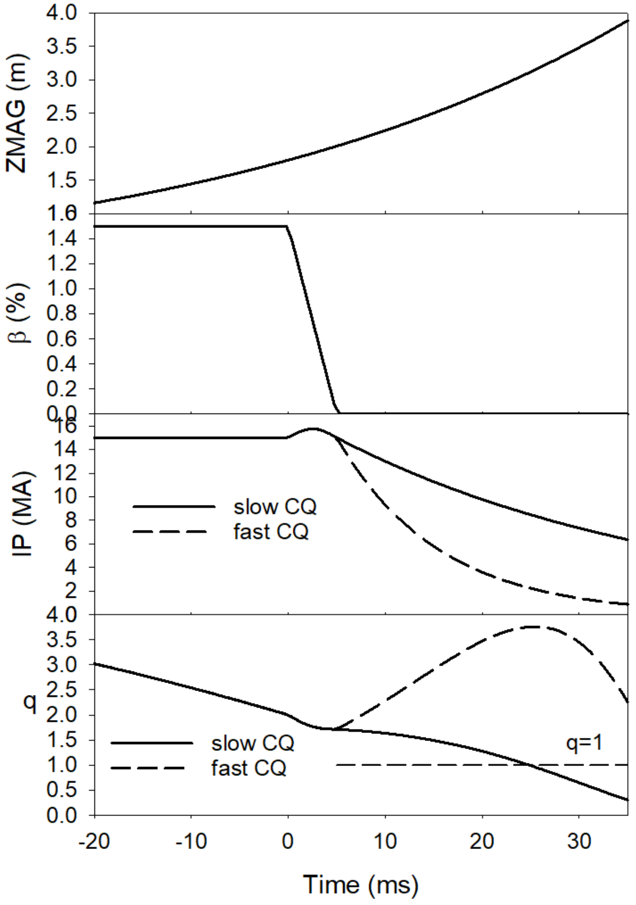

$$q(a) \cong 2\pi \frac{B_T a^2}{R \mu_0 I_p}$$

$$a = a_0 e^{-\gamma_{VDE} t}$$

$$I_p = I_{p0} e^{-\gamma_{CQ} t}$$

$$\frac{\dot{q}}{q} = \left[-2\gamma_{VDE} + \gamma_{CQ}\right]$$

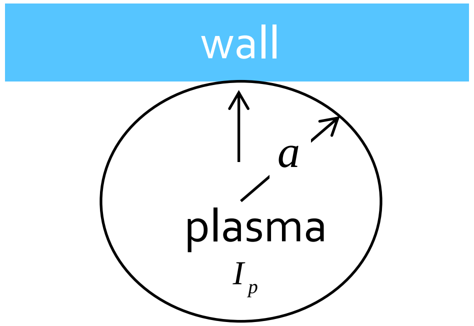

- If current decays too slowly so that $2\gamma_{VDE} > \gamma_{CQ}$ q(a) will decrease during the current quench, leading to q(a) < 1 ➔ large (1,1) mode and sideways force. Seen in JET and in modeling [1,2]
- However, in ITER, because the vessel is such a good conductor, the current quench time will always be less than the VDE time → q(a) will never go below 1 and a large horizontal force will not occur

Plasma contact with surfaces during VDE leads to "sheaths" that influence disruptive dynamics.

- Preferential loss of electrons induces electrostatic sheath layers.
- Magnetic field direction further influences the of outward flows.
- New sheath-based velocity boundary conditions investigated by PhD student, applied to NIMROD
  - $\boldsymbol{V}_B = \sqrt{\frac{T_e}{m_i}}\hat{\boldsymbol{b}}$
- Can have significant influence on plasma evolution during VDE as shown in temperature contours in figure

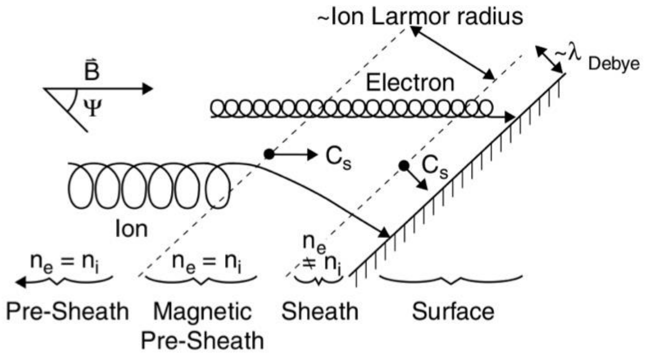

Mag. sheath sketch from P. C. Stangeby, *Pl. Bdry. of Mag. Fus. Devices* (Taylor & Fr., 2000).

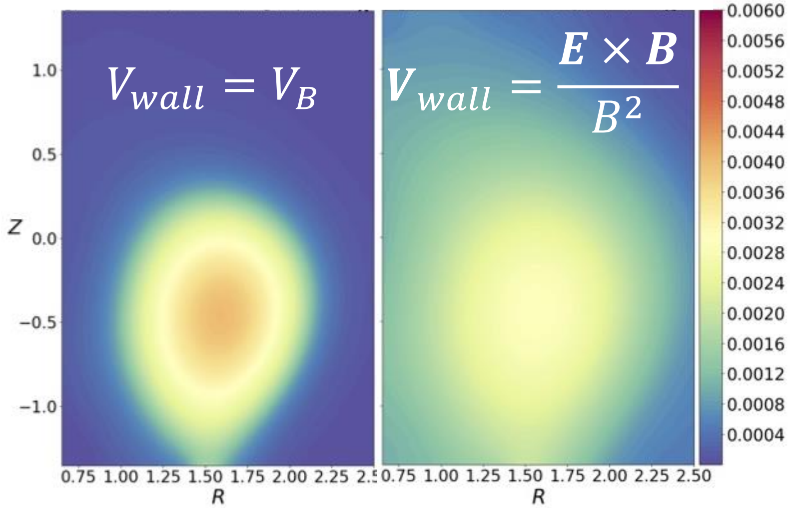

T_e profiles for computed VDEs indicate the influence of boundary conditions.

C. Sovinec
K. Bunders

M3D-C1 simulation of JET VDE shows origin and magnitude of sideways force – 2 (of 2)

- ΔF_{xC1} – sideways force as computed by M3D-C1
- ΔF_{NC1} – "Noll Force" approximation from M3D-C1
- $\Delta F_{N\,all}$ – "Noll Force" from all JET disruptions in 2011-16 ILW database
- $\Delta F_{N\,VDE}$ – "Noll Force" from JET VDE disruptions

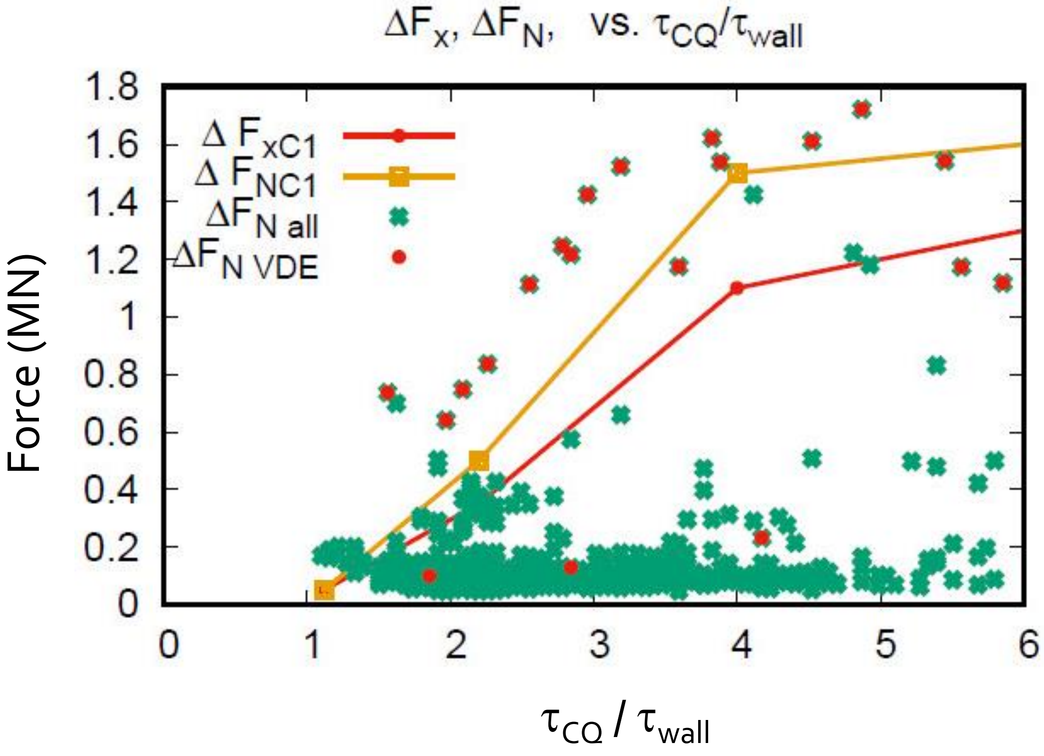

- JET uses an approximation to the actual force called the "Noll Force"
- M3D-C1 gives value for Noll Force mostly within 20% of experimental data using scaled values of τ_{wall}
- These are now being extended to use actual τ_{wall}

"Noll Force": $\Delta F_N = \pi B \Delta M_{IZ}$

4 time slices in a M3D-C¹ simulation of a 1 mm Carbon pellet injected into NSTX-U via EPI

Injection Plane Contours at different times

(a) 0.065 ms | (b) 0.324 ms | (c) 0.648 ms | (d) 0.973 ms

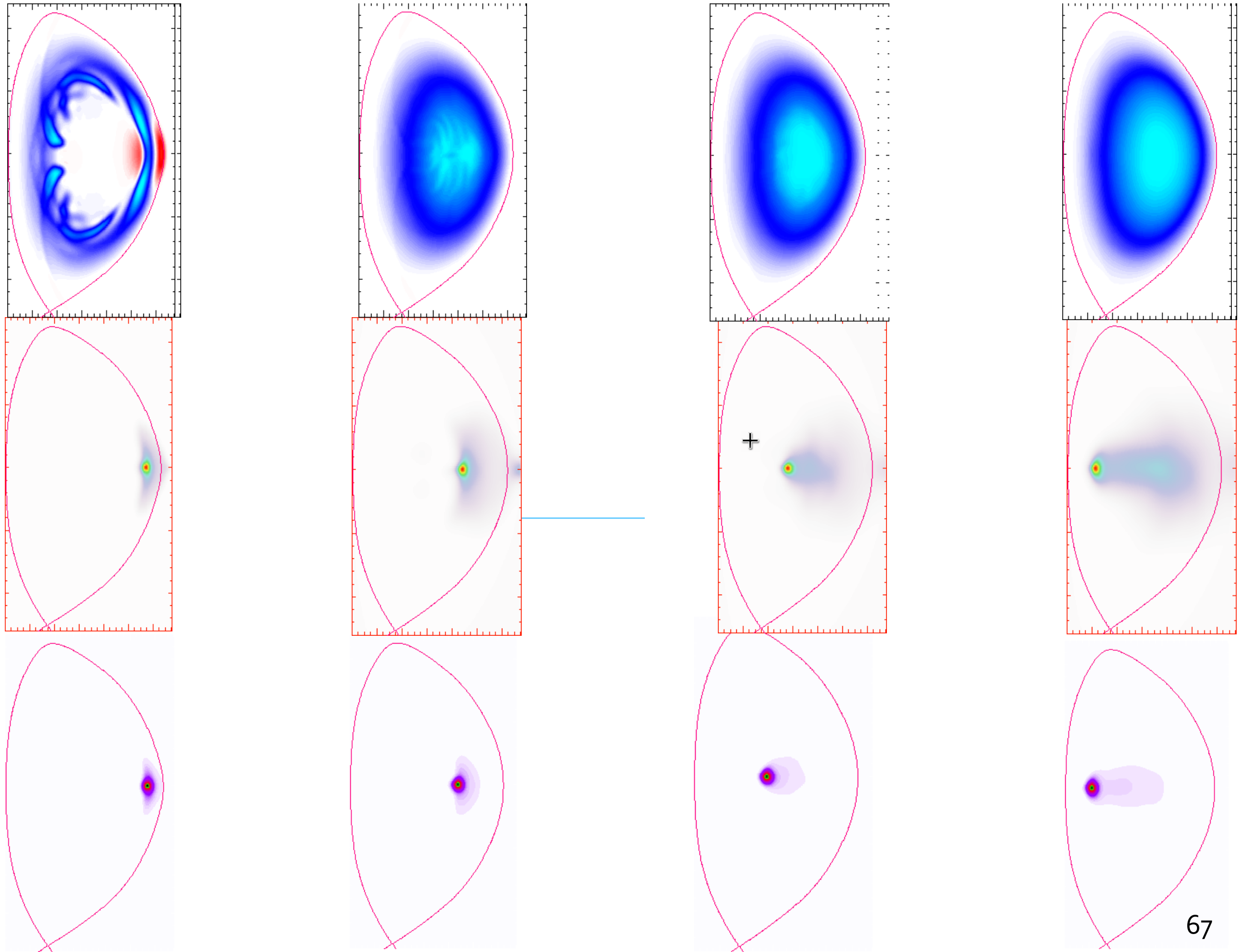

Change in Electron Temp.

(a) - 0.6 keV
(b) - 1.7 keV
(c) - 1.7 keV
(d) -1.7 keV

Carbon Density:

(a) 6.8 10^{19} m^{-3}
(b) 5.2 10^{19} m^{-3}
(c) 5.2 10^{19} m^{-3}
(d) 3.1 10^{19} m^{-3}

Radiation source:

(a) - 3.2. GW/m^3
(b) - 1.0 GW/m^3
(c) - 1.1 GW/m^3
(d) - 0.4 GW/m^3

Contours at t=0.13 ms at 4 toroidal locations for M3D-C¹ simulation of 1 mm Carbon EPI in NSTX-U

Same time (t=0.130 ms), different toroidal locations

(a) $\varphi = 0^o$ (b) $\varphi = 90^o$ (c) $\varphi = 180^o$ (d) $\varphi = 270^o$

Change in Electron Temp.

(a) – 969. eV
(b) - 1062 eV
(c) – 1034 eV
(d) - 1067eV

Carbon Density:

(a) 8.20 10^{19} m^{-3}
(b) 1.86 10^{19} m^{-3}
(c) 0.07 10^{19} m^{-3}
(d) 1.86 10^{19} m^{-3}

Radiation source:

(a) - 4400 MW/m^3
(b) - 40. MW/m^3
(c) - 0.5 MW/m^3
(d) -40. MW/m^3

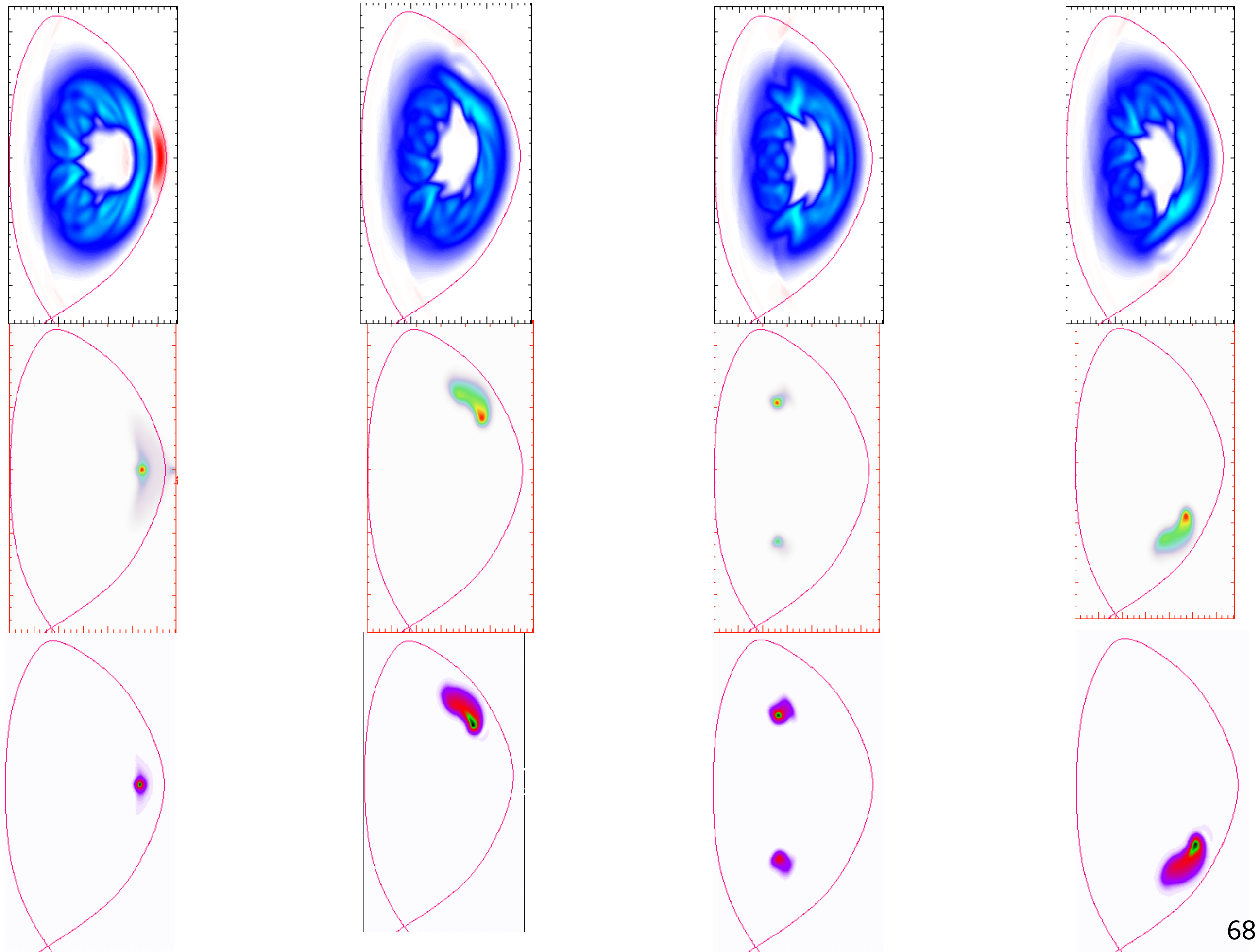

$\mathbf{V} = R^2\nabla U \times \nabla\varphi + \omega R^2\nabla\varphi + R^{-2}\nabla_\perp\chi$

Velocity Matrix Restructuring for Improved Preconditioning

- M3D-C[1] uses a physics-based Helmholtz-like decomposition of the velocity field:

$$\mathbf{V} = R^2\nabla U \times \nabla\varphi + \omega R^2\nabla\varphi + R^{-2}\nabla_\perp\chi$$

- The old ordering mixed these 3, physically different velocity variables in the same vector

- New ordering allows us to separate these, facilitating a more efficient pre-conditioning strategy.

(R,φ,Z) coordinates

Because each toroidal plane couples only to adjacent toroidal planes, the full velocity matrix is of block-tridiagonal form. Corner elements due to periodicity.

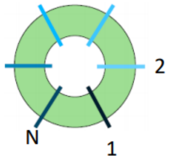

$$\begin{bmatrix} \mathbf{B}_1 & \mathbf{C}_1 & & \mathbf{A}_1 \\ \mathbf{A}_2 & \mathbf{B}_2 & \mathbf{C}_2 & \\ & \ddots & \ddots & \ddots \\ \mathbf{C}_N & & \mathbf{A}_N & \mathbf{B}_N \end{bmatrix} \bullet \begin{bmatrix} \mathbf{X}_1 \\ \mathbf{X}_2 \\ \vdots \\ \mathbf{X}_N \end{bmatrix} = \begin{bmatrix} \mathbf{Y}_1 \\ \mathbf{Y}_2 \\ \vdots \\ \mathbf{Y}_N \end{bmatrix}$$

$\mathbf{X}_j$ contains all the velocity variables on plane j

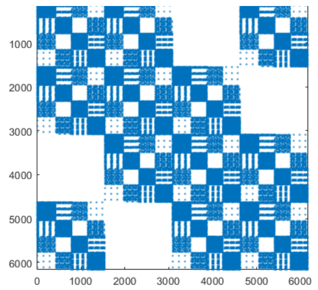

per-process

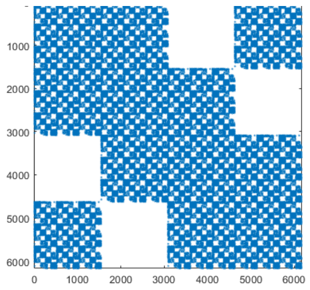

per-plane

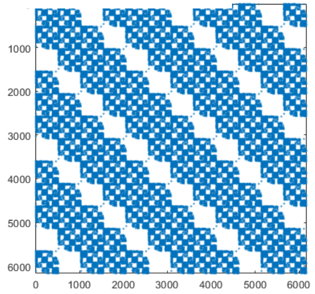

global